Aus der Universitätsklinik

für Zahn-, Mund- und Kieferheilkunde Tübingen

Abteilung Poliklinik für Zahnärztliche Prothetik und Propädeutik

Ärztlicher Direktor: Professor Dr. H. Weber

Sektion für Medizinische Werkstoffkunde und Technologie

Leiter: Professor Dr. J. Geis-Gerstorfer

Nano Hydroxyapatite/Collagen, Nano Hydroxyapatite and Anodic Oxides on Titanium

— Preparation, Characterization and Biological Responses —

Inaugural-Dissertation

Zur Erlangung des Doktorgrades

der Humanwissenschaften

der Medizinischen Fakultät

der Eberhard-Karls-Universität

zu Tübingen

vorgelegt von

Xiaolong Zhu

aus

Beijing, China

2005

Dekan: Professor Dr. C. D. Claussen

1. Berichterstatter: Professor Dr. J. Geis-Gerstorfer

2. Berichtersttater: Professor Dr. O. Eibl

Table of Contents

1 Introduction

Titanium is a successful biocompatible material that is extensively used for biomedical applications, especially for bone-anchoring systems, such as dental, orthopaedic implants and osteosynthesis applications. It has advantageous bulk mechanical properties such as a low modulus of elasticity, a high strength-to-weight ratio, and passive surface properties i.e. excellent corrosion resistance and low rates of ion release as well as a high degree of biocompatibility which is largely attributed to an inert surface oxide film [45, 71].

Bone formation induced by osteoblast-like cells at the implant-tissue interface is a complex process, involving a number of cellular functions such as cellular adhesion, migration and proliferation followed by the expression of markers of the osteoblast phenotype and synthesis, deposition, and mineralization of a bone matrix. Bone-implant interaction processes are, to a great extent, governed by surface properties of implant devices. A variety of surface properties including physicochemical as well as surface geometrical properties are believed to be responsible for the biological performance, i.e. cell attachment and subsequent osseointegration, of titanium implants [3,72]. The response of titanium to its biological surroundings is governed by ion leaching and by corrosion with the release of particles. These processes are not only dependent on solubility of the implant, but also on intercellular turnover, cellular activity, bacteria, pH, and other factors. The influence of the surface is particularly dominant during the early stages of biological response and it is also known that the very first biochemical interactions at the implant-tissue interface are decisive with respect to the course of later reactions and the final cell/tissue architecture of the interface. Besides, the fixation of implants either through chemical bonding or by mechanical locking for is determined by their surface properties, primarily topography and surface chemistry, which directly affect the interaction of implants and bones. Consequently, alteration of implant surfaces to promote titanium osseointegration, a process of the direct anchorage of implants by bone formation around the implants without any intervening soft or fibrous tissue [68], and their biological responses have been of a great interest in biomaterials, either from academic or industrial points of view.

1.1 Aim and content of the study

The purpose of the present study is to develop a new surface for titanium implants to optimize osseointegration at the bone-implant interface. Characterization and cell response of anodic oxides, nano HA and nano HA/collagen coatings will be investigated to understand cell reactions to their structures and chemistry. To improve the cell-titanium interaction, a certain approach will be searched to enhance hydrophilicity of titanium oxides.

The main content of the study includes:

(1) Preparation and surface characterization of anodic titanium oxides incorporated with P or Ca/P;

(2) Biological responses to topographies and compositions of titanium oxides including cellular viability, attachment and spreading, proliferation and differentiation;

(3) Ultraviolet light is employed to treat anodic oxides of titanium to enhance hydrophilicity;

(4) Correlation of structures and synthesis conditions of nano HA particles similar to bone minerals;

(5) Cellular reactions to nano HA particles and their effects of structures;

(6) Surface characterization and cell responses of nano HA/collagen coated on titanium and anodic titanium oxides.

The schematic flowchart of the study is shown as below.

```
┌─────────────────────┐          ┌─────────────────────┐
│      Titanium       │          │    Synthesis of     │
│                     │          │      Nano HA        │
└─────────┬───────────┘          ├─────────────────────┤
          ▼                      │    Structure &      │
┌─────────────────────┐          │    composition      │
│ Surface Preparation │          │  Characterization   │
└─────────┬───────────┘          ├─────────────────────┤
          │                      │    Nano HA sol      │
┌──────────┐  ┌──────────┐       ├─────────────────────┤
│   UV     │  │  Anodic  │       │       Nano          │
│treatment │  │ Oxidation│       │  HA/Collagen-Ti     │
├──────────┤  └──────────┘       └─────────────────────┘
│Wettability│
└──────────┘
          ┌─────────────────────────────┐
          │  Surface Characterization   │
          └─────────────────────────────┘
  ┌──────────┬──────────┬──────────┬──────────┐
  │Roughness │Morphology│Composition│Wettability│
  │          │  (SEM)   │  (XPS)   │(DSA, DCA)│
  └──────────┴──────────┴──────────┴──────────┘
          ┌─────────────────────────────┐
          │   Biological Responses      │
          │        (in vitro)           │
          └─────────────────────────────┘
  ┌──────────┬──────────┬──────────────┬──────────┐
  │Cytotoxicity│Cell adhesion│Cell proliferation│Cell Differentiation│
  └──────────┴──────────┴──────────────┴──────────┘
```

2 Some progress of biological performances and surface modifications of titanium

2.1 Characteristics and biological performances of titanium

2.1.1 Surface characteristics of titanium

Pure titanium exists as a hexagonal close-packed crystal structure (alpha phase) at temperatures up to 882°C and above that temperature up to 1665°C, body-centred cubic (beta phase). Commercially pure titanium (cp Ti) is available in four grades (grade 1-4) and contains dissolved oxygen, nitrogen, carbon, hydrogen and iron. Among them, the elements oxygen, carbon, nitrogen and aluminum play a role in stabilizing the alpha phase of titanium by increasing solubility in the hexagonal close-packed structure; while manganese, chromium, iron and vanadium stabilize the beta phase [91]. The electronic structure of titanium consists of $1s^2$, $2s^2$, $2p^6$, $3s^2$, $3p^6$, $3d^2$, $4s^2$, in which the lightly held $3d^2$ and $4s^2$ electrons are highly reactive, and thus titanium can spontaneously and instantaneously form a tenacious oxide, which varies both in thickness and composition under certain circumstances. The native titanium oxide film formed in air or water is typically 4-6 nm thick, amorphous or poorly crystallised. The oxide film on titanium is non-stoichiometric TiO_2, that is, predominantly TiO_2 with minor Ti_2O_3 and TiO.

As titanium is in contact with host tissues, it interacts with physiological fluids through its oxide film, which is responsible for corrosion resistance and biocompatibility. The surface oxide film has several oxides (TiO_2, TiO, Ti_2O_3) and among them TiO_2, the most common, is probably the most stable. TiO_2 exists as three crystalline forms including the orthorhombic brookite, the tetragonal anatase and rutile. However, the oxide film is not stable and grows in air, aqueous or physiological environments because of the highly defective structure of the initial thin film. From dynamics of the oxide growth, the oxide thickness with time follows the logarithmic law or the inverse logarithmic law and it is assumed that initial amorphous film is crystallized as the film thickness increases [45]. The explanation for the growth law is that the oxide possesses an amorphous structure at the initial stage with a high rate of thickening and the rate diminishes as crystallization occurs [113].

The chemical composition of the oxide film on titanium varies via the exchange with its surroundings. *In vitro* experiments indicate the incorporation of calcium and phosphate ions into the titanium oxide and it leads to the natural formation of a calcium phosphate layer similar to apatite [55]. It has been found that H_2O_2 generated by inflammatory response favours the incorporation of calcium and phosphate and precipitation of apatite [104]. The *in vivo* analyses of titanium implants demonstrate an unexpectedly high rate of titanium ion release [115], an oxide growth and incorporation of phosphate and calcium ions into the titanium oxide film in the human body [87].

2.1.2 Surface contamination

The titanium oxide surface has a strong affinity to both inorganic and organic contaminants from air or aqueous solution such as Fe, Zn, Sn, Pb, C, H, N, O. Therefore, surface contamination, for instance absorption of ubiquitous hydrocarbons to the surface of implants, is unavoidable and has been considered to be, in part, responsible for their poor performance *in vivo* [11]. Fe, Zn, Sn or Pb is believed to have contributed to the observed lack of osseointegration [8]. The presence of elements such as C, H, N and O affects the biological response of implants though the mechanism of the effect is not well known. Surface treatment processes of titanium determine the type and degree of the contamination. As a consequence, several surface contaminations occurring, as briefly described below, according to surface treatment methods.

Sterilization is an indispensable process for titanium implants before implantation. Steam autoclaving may produce organic contaminants on the implant surface. As to possible effects of autoclaving, there is some controversy whether the oxide layer on titanium implants is changed or increased in thickness. On one hand, Sterilized surfaces contain O, C, and N contaminants, which affect surface energetics and decrease attachment of cells to autoclaved surfaces but no significant effect on cell spreading [70]. On the other hand, it has not been also found any significant difference in thickness or binding energy of surface oxides on cp titanium before and after various steam

treatments [126]. By comparing different sterilization methods, it was shown that ultraviolet (UV) sterilized surfaces seemed no difference from the unsterilized state, and both ethylene oxide and steam autoclave sterilization contaminated and altered the titanium surface, resulting in decreased levels of cell attachment and spreading *in vitro* [126]. Whether multiple sterilization procedures have detrimental effect on final implant success is still not clear.

The absorption content of hydrocarbon on the surface of titanium implants increases with contact time with air. The contaminants of abraded Ti surfaces have oxygen and silicon, which is from a SiC sandpaper during polishing, leading to the increase of surface hardness [93]. In the acid pretreatment, the degree of sulfur on the surface treated depends on the concentration of the sulphate acid, and however, chlorine on the surface treated with HCl in any concentration is barely detected [122].

Since fibroblast adherence to titanium surfaces is impeded by endotoxin [102, 143], it is likely that it would be desirable to remove or decontaminate surface contaminants to obtain maximum osseointegration. Using strips of titanium either grit-blasted or coated with hydroxyapatite to treat contaminated titanium surfaces, it has been found that endotoxin could be removed most effectively using air-powder abrasive systems and bone filled in the peri-implant bone defects has been demonstrated by radiography [41, 105, 143], while citric acid is able to effectively remove contaminants at treating hydroxyapatite surfaces. By different cleaning tests on various implant surfaces contaminated with radioactive endotoxin, it has been shown that machined implants are more easily decontaminated than are titanium-plasma-sprayed and hydroxyapatite-coated implants, and an air abrasive system is the most effective, while chlorhexidine is the least effective. For biological contamination, it still has no satisfactory approach to clean even though multiple techniques have been tried such as ethanol rinsing, ultrasonic trichloroethylene (TRI) with ethanol, abrasive, supersaturated citric acid, CO_2-laser dry and wet conditions [88].

2.1.3 Effects of surface characteristics on biological responses

(a) Surface energy

The interaction between the outermost surface of a biomaterial and its environment is a highly dynamic process, in which protein adsorption is a key factor. Surface energy, initially, may play a major role in determining which proteins are adsorbed onto the surface, as well as whether or not the cells themselves adhere to the surface, and further influences the latter stage of bone formation and calcification through preferring the adhesion of some cell types [72].

Wettability, a measurement of surface energy, is often used as one of surface characteristics. Normally, the amount of adsorbed protein is higher on hydrophobic surfaces than on hydrophilic surfaces [79, 132]. However, strong hydrophobic, low-energy materials, e.g. polydimethysiloxane-pretreated surfaces, exhibited a low tendency to adsorb proteins due to energetically unfavourable conditions [15], and strong hydrophilic materials suppressed the protein film adsorption, probably due to the absence of both hydrophobic interactions and double-layer attraction forces [53], as protein adsorption depends on the magnitude of the interacting forces between the biomolecule and the surface. Cell adhesion, different from protein adsorption, occurs readily to hydrophilic surfaces but inefficiently to hydrophobic surfaces. Generally, surface energy is proportional to cellular adhesion strength, and thus, the metals of high energy have much greater adhesion strength of cells than the polymeric materials of lower energy. The clean titanium surface is hydrophilic due to the high polarity of the Ti-O bond and its surface contamination such as carbon or hydrocarbon adsorption produces high values of water contact angles. Surface energy can readily be changed by processing in the preparation of titanium implants. By glow charge, increased surface energy results in the increase of cellular adhesion [8]. Osteoclast differentiation is greatly activated by glow charge pretreatment [136]. Increased surface energy does not selectively increase the adhesion of particular cells or tissues, and it has not been shown to increase bone-implant interfacial strength [25]. By inserted in the rabbit tibia and femur, glow-discharge-treated implants demonstrated similar

early bone healing responses to those with the conventional implant treatment [22]. As the surface of the material is more or less inhomogeneous, surface energy alone is not enough to display the surface characteristics and postulate the interaction of cells and surfaces. On the other hand, surface energy is dictated by surface composition and topography (including roughness) of the implant.

(b) Surface topography

The response of cells and tissues at implant interfaces can be affected by surface topography on a macroscopic as well as a microscopic level. On the cell level, surface topography plays a fundamental role in regulating cell behaviour, e.g. the morphology, orientation and adhesion, proliferation and differentiation of mammalian cells [35]. The reaction of cells to topography of the substratum to which they are attached is one of the first phenomena observed in tissue culture and therefore play a major role in the evolution and the properties of the implant-tissue interface,e.g. osseointegration.

(i) Surface roughness

The titanium implant surface can be generally considered to be smooth and rough in terms of its roughness, i.e. the former average surface roughness Sa ≤ 1 µm while the latter Sa > 1 µm. Besides, Wennerberg et al. [134] suggested that roughness be described as smooth for abutments, whereas minimally rough for roughness 0.5 to 1 µm, intermediately rough for 1 to 2 µm, and rough for 2 to 3 µm. Cell responses to titanium surface characteristics have been shown to vary with cell types as well as cell maturation states. From *in vitro* to *in vivo* studies, a common agreement that greater initial cell attachment of osteoblasts on rough surfaces on titanium is accepted as the amount of roughness is within the dimension of individual cells [19, 34]. In contrast, more epithelial cells and fibroblasts were attached to the smoother surfaces than the rougher ones, and also the proliferation of these cells increased on the smoother surfaces [51]. By culturing rat calvarial cells on titanium surfaces in a range of Ra from 0.14 to 1.15 µm, the maximal attachment was demonstrated

on the surfaces with a Ra of 0.87 μm [19]. The effect of surface roughness on cell adhesion probably results from the fact that rough surfaces may adsorb more fibronectin, which, a cell adhesion protein present in serum, can mediate cell attachment and spreading on artificial substrates by interacting with glycosaminoglycans and the cytoskeleton [106], than smooth surfaces [131], preserving the synthesis of extracellular matrix proteins [90].

Morphology of cells varies considerably as surface roughness increases [4]. Cells on the smooth surfaces displayed flat, well-spread morphology, synthesized a collagen-rich matrix; while the cells on the rough ones assumed a round or cuboidal shape with cytoplasmic extensions communicating between cells or anchoring the cells to the peaks of the surfaces, and produced collagen-based matrix. The morphology of osteoblasts is related to their focal contacts, which distribute uniformly on all the membrane surfaces in contact with the substratum on smooth surfaces and visible only at the extremities of cell extensions where cell membranes are in contact with the substrate [73]. More cell spreading and continuous cell layer formation were shown on smooth surfaces compared to rough ones [73]. From chondrocytes on the same titanium surfaces, the effect of surface roughness on their proliferation is dependent on the maturation state of the cells [20]. The response of the less mature resting zone cells was comparable to that of MG63 cells, which is postulated to represent a relatively immature osteoblastic state. The more mature growth zone chondrocytes also exhibited decreased proliferation on rough surfaces. Using MG63 cells, Martin et al. [90] demonstrated cells cultured on rougher titanium surfaces exhibited decreased cellular proliferation and expressed more differentiated phenotype, which is a more osteoblastic phenotype. Besides, cells on the rougher surfaces were found to release higher levels of prostaglandin E_2 (PGE_2) and latent transforming growth factor β (LTGF β) [38], both factors involved in regulation of bone formation. However, some researchers showed osteoblastic proliferation could be enhanced on rough surfaces. All these contradictory data may be ascribed to the sensitivity of cells to the surface features, which are not sufficiently described by surface

roughness, implying that implant surface roughness modulates osteoblastic proliferation, differentiation, and matrix production *in vitro*.

In *in vivo* studies, a morphometric analysis showed increasing implant surface roughness generally correlated with increased surface coverage by bone. By evaluating different variables, Thomas and Cook [123] found that surface texture, i.e. a combination of topography and roughness, more than anything else, significantly affected the interface response to the implant. An implant with a rough surface yielded both greater shear strengths and direct bone apposition, whereas the implant with smooth surfaces exhibited various degrees of fibrous encapsulation. Therefore, rough surfaces are assumed to produce better bone fixation than smooth surfaces. It has been indicated that soft tissues interact better with smooth polished titanium surfaces, whereas rough titanium surfaces rather promote bone tissue formation and osseointegration [28]. On the other hand, an *in vivo* study showed that very different rough surfaces of titanium exhibited a similar bony reaction and no significant difference in the interface length percentage covered by bone [60]. Thus, the organisation of surface features also takes effect on bone formation at the implant-implant interface.

(ii) Surface structures

All anchorage-dependent cells, either *in vitro* or *in vivo*, have to contend with some substrate topography. Thus, reactions of cells to topographic cues are important for diverse processes *in vivo* e.g. morphogenesis, cell invasion, repair and regeneration [35]. Cells can discriminate not only between surfaces of different roughness, but also between surfaces even with comparable roughness but different topographies. The micron- and nano-topography can present strong cues for cell behaviour and thus, the interactions of cells with topographic features of the substrate they attach to will affect a variety of cellular processes such as cell adhesion, cytoskeletal organization, cell motility, migration patterns and cell differentiation [35, 36, 137]. The reactions of cells to the topography of their substratum, are assumed contact guidance, the phenomenon has been demonstrated by the organization of surface roughness. The tendency of surface topography to influence cell spreading is called

"contact cue guidance" [33]. Such effects depend on not only the size and structures of the features of the substratum but also the cell type. Curtis et al. [33, 36] have shown that cells align themselves with topographical features such as parallel grooves etched into a biomaterial surface. Certain cells, such as fibroblasts - cells responsible for producing extracellular matrix in wound healing and tissue remodelling - will migrate along the tracks. Others, for instance macrophages, will remain 'trapped' within the features. Epithelial cells were markedly oriented along the long axis of 10 μm deep grooves on titanium-coated implants [27]. On grooved surfaces, cells generally align to the long axis of the grooves [39, 40], and the alignment of cells with structures, e.g. grooves, walls and edges, is often accompanied by the organization of actin and other cytoskeletal elements such as microtubules in an orientation parallel to the structures [29, 138]. The analysis at the molecular level indicated F-actin condensations appeared at topographic discontinuities, often at right angles to groove edges, and some cells were observed to have lamellae and filipodia bending around edges. Among cytoskeletal elements, microtubules were the first element to align to grooves, followed by actin [138]. Bone cells on smooth surfaces were oriented randomly or ignored the surface topography on a 0.5-μm grooved surface and span the width of the groove but they are lined up parallel to the grooves in an end-to-end fashion in 5-μm-deep grooves [128]. By culturing rat dermal fibroblasts on microtextured silicone, polystyrene, titanium, or poly-L-lactic acid (PLA) substratum with 1, 2, 5, and 10 μm in width and 0.5, 1, and 1.5 μm in depth [23, 39, 129], it has been observed that the rate of orientation increased drastically when the grooves were made deeper, and however, the number of cells was not highest in the deepest grooves because the cells bridge the grooves [40]. Consequently, it becomes a common agreement that the depth of grooves is more important than their width in determining cell increasing orientation. If surface structures are far greater in size than cells, their effects on orientation of cells disappear. As the groove/ridge width is reduced to the size of the cells or less, the effects on orientation become more marked. As to other structures such as pores, much less attention has been paid than grooves. Cambell and von Recum [23]

examined the effects of pore size and hydrophobicity in their study involving a cannine *in vivo* implant model. They found that pore size played a larger role than material hydrophobicity in determining tissue response, with pores of 1-2 µm allowing for direct fibroblast attachment. A positive effect of the surface microstructure (pore diameter of 3-8 µm) on both osteoblast fixation and number has been also demonstrated [2, 56]. One probable explanation for increased cell growth is that a porous microstructure presents a stimulus to an orientated cell development [71]; while another is that porous surfaces have a larger culture surface and thereby a lower cell density than smooth surfaces [80]. However, on the smooth surface the cell proliferation was significantly higher in the early phases due to the faster growth. At later time points, the porous surfaces yield higher proliferation.

Although a great amount of work has been investigated into preparation and biological responses of different micron- and nano-structured surfaces [35], not much research have been done on structured surfaces and their cellular reactions of titanium because it is difficulty to apply structuring technologies to titanium surfaces. Anselme et al. [5] observed improved orientation, adhesion and proliferation of human osteoblasts on titanium surfaces with a micro-roughness (below the cell size) by a lower level in the organization of topography and by relatively high amplitude of topography. Human osteoblasts displayed oriented in a parallel order on polished surfaces and the orientation was not affected by residual grooves after polishing; while on the sandblasted surfaces the cells never attained confluence and had a stellate shape and cell layer had no particular organization [73]. Keller et al. [71] have shown that the highest level of rat osteoblast cell attachment was obtained with rough, sandblasted Ti6Al4V surface compared to grooved ones although their Ra values were identical. The reaction mechanism is probably that the sandblasted surface is highly irregular in morphology with many small flatter-appearing areas of various sizes, so that the sandblasted surface may provide a more available area or for attachment of not only cells, but also the extracellular matrix (or preconditioning protein layer) required by the cells for attachment. Therefore,

both surface roughness, Ra values, and micro-morphologic patterns (irregular or regular) affect cellular responses.

The osteoblastic response differs significantly with very small porous surface difference. Stangl et al.[117] investigated cell adhesion of osteoblastic cells on cp Ti implants with a series of porous geometries and they postulated that an increase in surface area was not the deciding regulating factor of cell growth at the bone-implant interface, and the implant microstructure was of importance. For bony ingrowth, the favorable surface pore sizes are in the range from 10 to 500 μm although a border level of 75 μm has been identified in some studies [75]. Li et al. [80] suggested that a porous surface with pore diameter of 140 μm have maximal bony ingrowth. Homsy [58] described a 300 μm pore size as the most favourable and Pilliar [110] proposed that a minimum pore size of 50 μm be used. Porous diameters of 200-400 μm have long been preferred and it is suggested such diameters produce optimal cell migration cell migration, adhesion and cellular proliferation [97]. The size (100 μm) of pores is widely quoted as the border level for pore diameter when considering bony ingrowth in minerealized bone. An increase in the surface area of the porous surface alone is not responsible for an increase in cellular proliferation, cell vitality or cell synthesis capability.

2.2 Surface modifications for titanium

The stability of an implant is determined by their osseointegration, which in large part depends on the chemistry and topography of its surface. Although the surface oxide film on titanium can be healed by itself within milliseconds, the dissolution of metal ions during its regeneration into the human body can induce the release of potentially osteolytic cytokines involved in the implant loosening [47]. Besides, the healing process of the interface between titanium and hard tissues, or osseointegration, is slower and the fixation of the titanium implant with host tissues is rather weak. Surface modification can alter the surface topography and chemistry, which directly affect the biological reaction to implants, that is, the interaction of implants and biological environments. A number of surface modifications and strategies have been developed to

improve the osseointegration of titanium implants and can be divided into physical and chemical treatments as well as a combination of both. Some of them are summarized as below as well as in Table 1.

Machining, in fact, not a method of surface modification, influences the topography and composition of titanium [71]. Oriented grooves, surface stress, metallic debris are produced on the surface of titanium during machining. Besides, the surface of titanium is probably contaminated by absorption of hydrocarbon from air and other organic substances from cleaning solvents.

Blasted surfaces are produced using an appropriate blasting medium such as hard particles of different sizes and shapes SiC, Al_2O_3, SiO_2, ZrO_2, TiO_2 and calcium phosphate. The topography of blasted titanium surfaces contains irregular pits and depressions, depending on blasting conditions, e.g. blasting medium and time, air pressure and distance from nozzle to target surface [110]. Blasted surfaces with modified topographies have graded stress, structure and composition to the substrate. Since some blasting medium is likely to be embedded in the implant surface, two measurements have been often taken to avoid possible negative effects due to residual blasting medium. One is to remove the residual particles by chemical treatment, e.g. ultrasonic cleaning with acid and alkali solution; the other is to use biocompatible or bioactive particles SiO_2, TiO_2 and calcium phosphate. To modify surface topography and chemistry of titanium, blasting is often combined with other treatments such as acid etching.

Acid etching is frequently employed to develop porous surfaces for enhancing implant fixation in bone. Acids commonly used for titanium surface etching consist of HNO_3 and HF, or HCl and H_2SO_4. The advantage of porous surfaces by acid etching is a continuous part from the substrate or no remarkably layered structure with the underlying substrate. Acid etching is usually combined with some physical manipulations e.g. sandblasting, machining or plasma spraying, also as a preceding for alkaline treatment.

Alkaline treatment is to create bioactive layers on titanium surfaces by immersing them in thermal NaOH solution and subsequent heat treatment. The surface layer consists of an irregular and porous sodium titanate and TiO_2 (rutile)

[74]. Alkaline treatment generally includes immersion in 4-10 M NaOH at 60 °C for 24 hours and then heat treatment at 600 or 800 °C for 1 hour. Alkali and subsequent heat treatment probably cause low adhesive strength at the interface of the treated layer (about 1 μm in thickness) and the substrate by distinct structures and compositions.

The increase of thickness in surface oxides on titanium is an efficient method to stabilize the oxides. To do it, two approaches are considered i.e. thermal oxidation and electrochemical oxidation or anodic oxidation. The thermal treatment by heating in air at 400-600 °C or in deionised boiling water for several hours produces a thin surface oxide layer (about 30-100 nm in thickness) [81]. Thermal oxidation is very limited in thickening surface oxides of titanium. In contrast, anodic oxidation is able to not only enhance the thickness of surface oxides on titanium but also modify their composition and topography efficiently. The development of electrolytes can be divided into two types, i.e. one is composed of dilute acids such as H_2SO_4, H_3PO_4, acetic acid and others only for thickening surface oxides [1, 146], and the other is involved in incorporation of some elements such as calcium and phosphorus into surfaces of titanium [145, 147]. Anodic oxides vary in thickness from 10 to 2000 nm, in topography from smooth to porous structure and in composition as expected to incorporate Ca and P with controlled content. There is a tightly adherent strength, affected by electrolyte and electrochemical parameters, between anodic oxides and the substrate. Anodic oxides containing Ca and P are further processed by hydrothermal treatment to join bioactive coatings on or in the surface.

Hydrothermal treatment is a physical-chemical process based on the relation of temperature, relative humidity and time. By utilizing the composition of solution or/and surfaces of titanium, calcium phosphate or calcium titanate is synthesized by hydrothermal treatment. For hydrothermal treatment, typically, necessary compositions such as calcium and phosphorus are generally from solution, which provides compositional sources for hydrothermal coatings. CaO and $CaCl_2$ solution are used as hydrothermal media to form calcium titanate on titanium surfaces [54]. In recent years, calcium and phosphorus as a

subsequent composition source are imported into titanium surfaces by anodic oxidation [148] or ion implantation [108]. Hydroxyapatite coatings or needles are synthesized on anodic oxides of titanium. Either calcium titanate or hydroxyapatite formed by hydrothermal treatment is brittle and its distribution and thickness in the surface are difficult to control. Besides, the interfacial strength at coatings and titanium substrate is weak. Hydrothermal-electrochemical deposition to form hydroxyapatite coatings probably improves surface homogeneity [13], but the effect is very limited.

Sol-gel have been increasingly become an important approach to synthesize thin ceramic films or coatings (< 10 μm in thickness) on implant surfaces to improve their biological performance. Films or coatings derived from sol-gel are easy to be prepared either on titanium surfaces or on modified titanium surfaces and convenient to control their composition, structure and homogeneity due to precursor mixture at the molecular level in solution. Ceramic coatings for titanium implants can be divided into three basic types, that is, titania, bioglass and calcium phosphate according to their compositions [42, 92, 99]. Composite coatings often consist of TiO_2-SiO_2, TiO_2-(hydroxy)apatite, or glass (SiO_2)-(hydroxy)apatite, [92]. The sol-gel-derived coating can be further tailored to obtain gradient properties. However, the adhesion between the coating and titanium substrate is still open to improve.

Biological systems are known to control the nucleation processes by means of genetically assembled organic functional groups [16] and crystals grown through adsorption of water-soluble polymers on certain crystal surfaces. The biomimetic approach is to utilize processes of physical chemistry to synthesize inorganic materials. Biomimetic synthesis of hydroxyapatite on titanium surfaces is performed frequently in simulated physiological solution. To induce the nucleation of hydroxyapatite, it is believed a key to create Ti-OH groups or triple bond Si-O(-) on titanium surfaces. Different methods have been employed as pretreatment for titanium to produce Ti-OH groups such as H_2O_2, NaOH, plasma spray, sol-gel and electrochemical oxidation [67]. The approach has a very slow precipitation rate of hydroxyapatite, and the precipitated layer is loose but can be used to form bonding with bone.

To coat calcium phosphate on titanium surfaces, there are a number of techniques besides those mentioned as above. Among them, thermal (plasma) spraying of calcium phosphate (30-200 µm) onto titanium surfaces is the most widely used technique and have been clinically applied though some disadvantages occur such as decomposition of calcium phosphate and the weakening of interface of coatings and substrate due to high temperature and rapid cooling speed. Electrochemical deposition (0.1-2 µm) [13], sputter coating (0.02-1 µm) [139] and pulsed laser deposition (0.05-5 µm) [83] are suitable for the simple-shape surface and micro-cracks are difficult to avoid in the electrochemical coating. Dip coating (0.05-5 mm) is generally inhomogeneous in thickness and becomes weak in adhesive strength during subsequent adverse effect of the high-temperature sintering cycle on the mechanical properties of titanium [83]. Till now, there is no technique to achieve satisfactory coatings of calcium phosphate on titanium implants.

The linkage of biomolecules onto titanium surfaces have raised more attention to biofunctionalize the surfaces. The immobilization of biomolecules in titanium surface to control the adhesion of specific cells can be achieved by either physical adsorption or chemical binding. Physical adsorption is simple and reversible, and often allow for the retention of biomolecular activity. Chemical binding is by the covalent attachment of biomolecules to titanium surfaces through a coupling agent or layer, and mainly has four approaches, that is, silanizations, photochemistry, electrochemistry and self-assemble monolayers (SAMs). There is an excellent review on biochemical modifications of titanium [140]. Biomolecules linked onto titanium surface primary actually affect the process of cell-surface interactions, and however, no evidence has been shown to promote the fixation of implants.

Table 1 Surface modifications and surface properties of titanium

Surface modifications	Surface composition	topography	Refs
A. Physical manipulations			
1. Mechanical processing			
Machining	TiO$_2$ with contaminants, e.g. C,H, N,O or Si	Grooved with parallel machining lines, pits, gouges, protrusions; roughness (Ra): 0.3-0.6 µm.	[71]
Polishing			
polishing media:SiC, Al$_2$O$_3$, diamond	TiO$_2$ with C, N,O, Si, or Al	Smooth surfaces; rougness (Ra): 0.1 µm or less	[71]
Shot- or grit-blasting, e.g. SiC, Al$_2$O$_3$,	TiO$_2$, HA with Al, Ti, ceramic particles	Depressions, gouges produced by plastically defomation; Roughness (Ra): 0.5-6 µm.	[50, 135]
2. Plasma treatment			
Ion implantation, e.g. N, O, Ca, P	TiN or TiNx, TiO2 with Ca or/and P	No marked change in topography,	[77, 98]
Plasma cleaning, e.g. Ar, O	TiO$_2$ inorganic contaminants, stoichiometric TiO$_2$		[6]
Plasma spraying	Calcium phosphate coatings	Porous surfaces	[120]
Plasma sputtering	Thin films of calcium phosphate	Smooth surfaces	[144, 83]
3.Laser treatment			
Laser cladding	Calcium phosphate coatings		[86]
Pulsed laser deposition	Calcium phophate films	Spheroidal micro- and macroparticles	[46]
Laser ablation	Calcium phosphate coatings	Grain-like particles or droplets	[12, 46]
4. other methods			
Ion sputtering	Thin calcium phophate films		
Magnetron sputtering	Thin calcium phosphate films		
Thermal oxidation	TiO$_2$	No influence on topography	[81]
B. Chemical manipulations			
1. Acid etching	Titanium oxides with residual elements, e.g . S, Cl, F, N.	Etched pits, dimple-like depression,	[30]
2.Chemically treating			
H$_2$O$_2$; CaP;	Ti-OH groups; CaP layer	Microporous layer	[133]
3. Alkali- and heat-treating	Ti-OH groups		
4. Anodic oxidation	TiO$_2$ with S, P or Ca/P	Smooth or porous surfaces	[1,145-147]
5. Hydrothermal treating	Calcium phosphate	Needles on the surface,	[55, 148]
6. Electrochemical deposition	Calcium phosphate	Smooth surfaces	[13]
7. Biomimetic processing	Calcium phosphate	Flake-like structured surfaces	[67]

2.3 Biological responses to modified titanium surfaces

The chemical composition of implant surfaces is often different from the bulk of the material and depends on the processing and surface treatment of the material. As shown in Table 1, surfaces with different compositions on titanium have been developed by various techniques. In the present part, we try to briefly summarize effects of the surface composition by surface modifications on biological performances of titanium surfaces.

Effects of compositions of titanium oxides Elements such as C, O, S, Cl, N, P and Ca can be incorporated into surface oxides on titanium by oxidation medium, etching solution and ion implantation. The import of some compositions into the surface oxide alters surface physicochemical characteristics such as surface energy. C, O, and N imported to surfaces of titanium demonstrated improved bone integration [77], and this effect is different from the corresponding contaminated elements as discussed in 2.1.2. The surface oxides containing S, Cl, P and Ca displayed good cytocompatibility *in vitro* [77, 116] and enhanced bone contact and greater new bone apposition, particularly Ca [119].

Effects of coating compositions on titanium surfaces *In vitro* and *in vivo* studies show ceramic coatings better biological response than cp titanium surfaces. TiO_2 coatings by sol-gel or deposition consist of rutile and anatase and, comparing to natural TiO_2, show enhanced bone-like precipitation at the surface in a simulated body fluid [65]. Nanostructured TiO_2 films coated on titanium indicated positively effect on the osseointegration rate of Ti implants and the bone mineralization at the bone-coating interface *in vivo* [49]. However, no chemical bonding is formed at the surface of TiO_2 coatings, that is, TiO_2 coatings can improve biocompatibility but no bioactivity.

Silicon-based compounds possess the ability to bond directly to bone and include two families, i.e. the bioactive glasses and the glass ionomers. Glass coatings not only enable titanium implants to bond with bone and but have also some advantage, i.e. osteoinduction, over hydroxyapatite. SiO_2 as a main component play a key role in biological behaviours of glass caotings *in vitro* [111] and *in vivo* [63]. Silica is found to form a low solubility matrix in which the

network of silicate chains acts as a framework for ionic species (Ca^{2+}, PO_4^{3-}, Na^+, etc.), whose role is to stimulate the biochemical environment surrounding the bioactive glass and accelerate the nucleation of hydroxyapatite. Within silica-rich gel, Ca^{2+} and PO_4^{3-} are combined to form crystals of hydroxyapatite (HA) similar to that of bone, hence a strong chemical bond, due to the presence of hydroxyl groups (SiOH). Hench et al. considered this silica layer produced in bioglasses is flexible enough to provide the oxide-oxide spatial requirements to match the bone lattice, thus providing epitaxial sites for bone growth [57]. Bioactive glasses have been found to stimulate genes in osteoblasts [141], causing upregulation of various osteoblast-specific genes.

Calcium phosphate compounds are abundant in natural and living systems. Calcium phosphate compounds vary in composition e.g. with minor CO_3^{2-} or F^-, and structure. Hydroxyapatite, calcium phosphate most extensively used for bone repair, coated on titanium has been shown to favour cell adhesion, differentiation and mineralization, and bone integration of implants compared to uncoated titanium due to the osteoconductive properties of HA [125]. The favorable effect of calcium phosphate coatings on bone response is explained by the hypothesis that dissolution and reprecipitation of calcium ions from the coating stimulates osteogenic cells to differentiate and deposit a mineralized matrix [107]. It can therefore be expected that new bone will form directly on the surface of the HA coating. HA coatings with high degrees of crystallinity show low-dissolution rates *in vitro* [85] and less resorption and more direct bone contact *in vivo* [76]. However, HA coatings with high amorphous contents result in rapid weakening and disintegration of the coating and often promote inflammatory responses in the surrounding tissue.

In vitro investigations demonstrated a great similarity in morphology of osteoblasts cultured on HA and uncoated titanium [14], and more spreading of osteoblasts on uncoated titanium comparing to those on HA. Okumura *et al.* [101] suggested that the lack of vinculin-containing adhesion sites in the osteoblasts on HA was because they were of a more differentiated phenotype. Okamoto et al, however, reported that a significantly higher number of cells adhered to HA than to uncoated titanium [100].

In vivo studies showed that HA coatings enhanced bone healing at the gaps between the bone and implant surface and hydroxyapatite coatings permitted an implant fixation far superior to current methods using either cemented or cementless techniques [26]. On the other hand, controversial clinical reports indicated that the HA coating did not provide any clinical or radiographic advantage over titanium [95, 142].

The crystallinity, composition, morphology and particles sizes of calcium phosphate affect its dissolution, which may explain the significant controversy concerning biological performances of calcium phosphate coatings either *in vivo* or *in vitro* studies [2, 95]. Although a number of physical and chemical techniques for preparing HA or Ca/P overlayers for titanium implants have been explored [52, 124], each method has some disadvantages. For example, as one of the most accepted alternatives, a plasma-spraying technique to deposit hydroxyapatite (HA) coating on titanium still has some drawbacks, i.e. HA is heated to above $10^{4\circ}C$, whence it suffers thermal decomposition forming tricalcium phosphate and tetracalcium phosphate, and may also form amorphoous phase on the interface between the coating and the substrate, and the adhesion of the interface is difficult to control.

In recent year, nanotechnology has been applied to produce nano HA coatings on titanium surfaces, including sol-gel, chemical coprecipitation, biomimetic synthesis and physical deposition. It is expected to have promising biological performance for nano HA coatings. The dissolution law of nano HA shows very different from that of conventional HA, and the particle-size effect is dominant for the dissolution of nanoscale HA [56]. Biological response to nano HA has not been reported, and investigations into a new coating of nano HA and its biological behaviour should be of interest for the potential application of nano HA in medicine and dentistry.

In summary, since the clinic success of orthopaedic and dental implants largely depends on the osseointegration at the bone-implant interface, surfaces of bone-contacting devices would be desirable to be compositional, structural and functional analogues of bone. To endow titanium with bioactivity, bonds must be

formed between its surface and living bone. Among the artificial materials known to be bioactive, HA, chemically and structurally similar to the minerals of bones and teeth, is known to enhance bone formation and is employed for hard tissue repair and augmentation of living bone. Synthetic HA exhibits strong affinity to host hard tissue, promote osseointegration and expedite the healing period required for titanium implants though its poor mechanical properties. It is known that bone consists of roughly 70% hydroxyapatite mineral and an organic matrix consisting largely of collagen type I, which is the principle collagen of skin and bone. Recently, researchers tried to coat titanium alloy with collagen type I to investigate its beneficial effect in osseointegration. It is demonstrated that the initial adhesion and spreading of osteoblasts have been accelerated [48]. Although collagen supports adhesion of cells, and however, to enhanced bone mineral deposition still requires HA. Due to titanium implants have no bone-bonding ability, it would be one of the most promising approaches for bone-contacting implant surfaces to be designed to be similar to bone. Therefore, nano HA/collagen coated on surfaces of titanium implants to mimic bone would have a great potential to improve osseointegration.

To coat HA/collagen on titanium surfaces, two challenges would be met, that is, one is how to homogeneously mix nano HA with collagen without denaturing collagen and the other is how to strongly adhere nano HA/collagen to titanium substrate. Two measurements will be taken i.e. mixing neutral nano HA sol with collagen at a room temperature to achieve homogenous mixture at the molecular level without denaturisation of collagen, and microporous surfaces created on titanium by anodic oxidation as an intermediate layer to connect both the underlying substrate and HA/collagen. Since the anodic oxide are grown directly from the substrate, and the adhesion strength of the interface is found strong [1, 145]; on the other hand, the composition and structure (e.g. surface pores and crystallinity) of the anodic oxide can be controlled by regulation of electrolyte and electrochemical parameters [145, 146]. Consequently, anodic oxides can provide a gradient in composition, structure and mechanical properties from titanium substrate to nano HA/collagen.

3 Materials and Methods

3.1 Anodic oxidation of titanium

Rectangular specimens 20×10×1 mm in size were cut from a cp titanium plate (ASTM B265 GR. 2/TITANIA Products, Essen, Germany). The pretreatment procedure was that specimens were mechanically polished, cleaned by mixed HF/HNO$_3$ solution, rinsed with ethanol and deionised water, and subsequently air-dried. Anodic oxidation was performed in a galvanostatic mode with a current density of 70 A/m^2 using either 0.2 M H$_3$PO$_4$ solution [146] or a mixture of 0.03 M calcium glycerophosphate (Ca-GP) and 0.15 M calcium acetate (CA) as the electrolyte [145]. The temperature was maintained at 20°C by water bath during anodic oxidation. Immediately after anodic oxidation, specimens were rinsed with deionised water and dried with nitrogen gas. The group numbers of the specimens were assigned to the different processing conditions as follows.

G-1: pretreated Ti as a control;
G-2: pretreated Ti and anodised in 0.2 M H$_3$PO$_4$ till 200 V;
G-3: pretreated Ti and anodised in 0.2 M H$_3$PO$_4$ till 300 V;
G-4: pretreated Ti and anodised in 0.2 M H$_3$PO$_4$ till 350 V;
G-5: pretreated Ti and anodised in 0.03 M Ca-GP and 0.15 M CA till 140 V;
G-6: pretreated Ti and anodised in 0.03 M Ca-GP and 0.15 M CA till 200 V;
G-7: pretreated Ti and anodised in 0.03 M Ca-GP and 0.15 M CA till 260 V;
G-8: pretreated Ti and anodised in 0.03 M Ca-GP and 0.15 M CA till 300 V.

3.2 Synthesis of nano HA and structure characterization

3.2.1 Synthesis of nano HA

A calcium compound and a salt containing phosphorus (both were of reagent grade) were purchased from Sigma-Aldrich Chemie GmbH (Steinheim, Germany) and used as precursors. Both the precursors were dissolved in deionized water and then vigorously stirred (at the rate of 700 rpm) with a molar

ratio of Ca/P = 1.67 to achieve HA sol. Furthermore, the mixed solution was aged at 25, 50, 100 °C for 0, 24, 48, 72, 120 and 300 hours, respectively. After filtered and washed several times with deionized water, the mixture was dried at 25 or 70 °C for 24 hours, and finally powders were obtained.

The powders, synthesized with an aging condition of 100°C for 48 hours, were further annealed at 500, 700 and 900 °C.

HA sol, after aged at 100°C for 48 hours, was coated on cp and anodized titanium and dried in air for 24 hours.

3.2.2 Structure Characterization of nano HA

To analyse structures of nano HA particles, HA powders were mechanically ground and examined by XRD. The crystallite size of nano HA particles was semiquantatively calculated according to the Scherrer equation according to the (002) peak.

The powders were ultrasonically dispersed in acetone to form very dilute suspensions and then a few droplets were dropped on copper grips with a carbon-coated film. The observation of morphology and electron diffraction of structures were performed in a TEM at 200 keV.

3.3 Preparation of HA/collagen

Nano HA sol was synthesized as described in **3.2**. After aged at 100 °C for 48 hours, nano HA sol cooled to the room temperature in air. Collagen type I (calf skin), obtained from Fluka (Deisenhofen, Germany). was dissolved in 0.1 N acetic acid and the solution diluted by triple-deionized water. Furthermore, nano HA sol and dilute collagen solution were homogeneously mixed to obtain a nano HA/collagen sol, which was then coated on the surfaces of cp Ti, and anodic oxides containing P or Ca/P. The specimens coated with nano HA and nano HA/collagen were numbered as follows:

G-1-HA: G-1 with nano HA coating;

G-1-HC: G-1 with nano HA/collagen coating;

G-3-HA: G-3 with nano HA coating;

G-3-HC: G-3 with nano HA/collagen coating;

G-7-HA: G-7 with nano HA coating;

G-7-HC: G-7 with nano HA/collagen coating.

The schematic flowchart of synthesis, characterization and biological performances of nano HA and nano HA/collagen is shown in Fig.1.
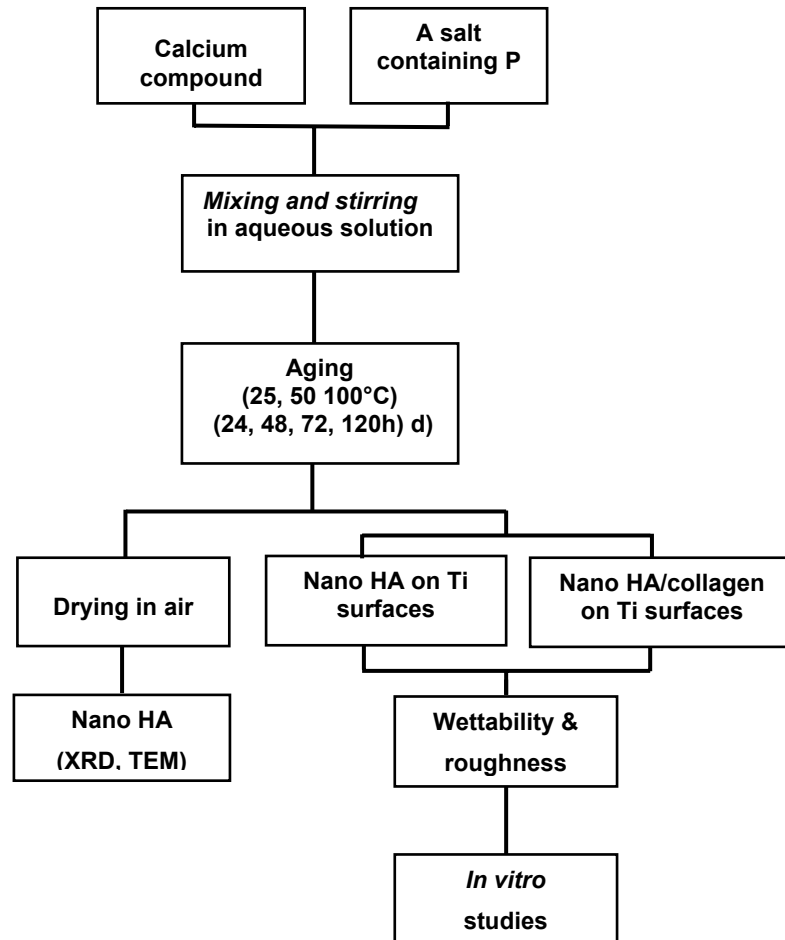

Figure 1   Schematic flowchart of synthesis,characterization and biological responses of nano HA and nano HA/collagen

3.4 Surface characterization

The surface roughness of the prepared specimens was quantified using a surface profilometer (Perthometer S6P, Perthen Instruments, Mahr, Goettingen, Germany). A 2 μm diamond stylus was used to determine the centreline average roughness along a 5.6 mm scan. The surface roughness of each

specimen was characterized by performing five individual equidistant line-scans being 200 μm apart. Twenty-nine parallel specimens for each condition were measured. The arithmetical mean (roughness average = R_a) of the surface roughness of every measurement within the total distance were assessed.

To observe the topography of the prepared specimens, they were coated with a thin plasma-deposited Au-Pd layer to avoid electrostatic charging during the measurement of scanning electron microscopy (SEM) using a Leo 1430. The average diameter of pores was determined from ten individual measurements.

Surface composition and elemental states of prepared specimens were determined quantitatively with VG ESCALAB 200 X-ray Photoelectron Spectroscopy (XPS) using a Mg anode.

The contact angle can characterize the wettability of the surface of a solid by a liquid, i.e. the interaction between a solid and a liquid surface at the interface, and represent a thermodynamic relationship known as the Young equation, which relates the angle θ to the interfacial solid-vapor (SV), solid-liquid (SL) and liquid-vapor (LV) free energies (γ) as follows: $\gamma_{SV} = \gamma_{SL} + \gamma_{LV}\cos\theta$.

Prepared specimens were kept in air for more than two months so as to stabilize the contact angle. Contact angles were measured on DSA 10 Mk 2 (Kruess) equipped with a video-imaging system. Sessile deionised-water drops were placed on the surface in the ambient environment, with drop volumes of 5 μl. Images were recorded during 1 min and 5 images every second with a video system, and the contact angle values were calculated by analysing drop shape using the Drop Shape Analysis System (DSA 1) and selected at 10 seconds.

Contact angles were measured before UV-treatment and at 2 hours after UV-treatment. UV-irradiation was performed for 1 hour under two 254 nm UV-light bulbs (Philips UV 15W/G15 T8 UV-C) at a distance between specimens and source light of 13 cm.

3.5 Cell culture and evaluation

3.5.1 Cell culture

The SaOS-2 human osteoblast-like cell line, derived from a human osteosarcoma, was obtained from the German Collection of Microorganisms

and Cell Cultures. The cells were cultured in a modified McCoy's 5A medium (Sigma-Aldrich Chemie GmbH, Taufkirchen, Germany) containing 10% fetal calf serum (FCS; PAA Laboratories GmbH, Linz, Austria), 1% penicillin (10,000 units)/streptomycin (10 mg/ml, GIBCO, Scotland, UK) and 1% 200 mM L-glutamine (PAA Laboratories GmbH, Linz, Austria) and maintained in an humidified atmosphere containing 5% CO_2 at 37 ºC. The culture medium was renewed twice per week. When cells reached confluence, a diluted Trypsin-EDTA (0.5g/L Trypsin and 0.2g/L EDTA, GIBCO, Scotland, UK) was used to detach cells from the bottom of the culture flasks, and 1/3 of the total cells were transferred into a new tissue culture flask.

3.5.2 Cytotoxicity

Cytotoxicity tests were performed by an extract method. Extracts of all specimens were obtained from contact of samples with modified McCoy's 5 A cell culture medium for 72 h at 37ºC (according to ISO 10993-5).The ratio between sample surface and the volume of the extraction vehicle was 3 cm^2/ml. SaOS-2 osteoblast-like cells at a concentration of 5000 cells/well were seeded in a 96-well plate in 150 µl modified McCoy's 5A medium per well. After 24 h the medium was discarded and replaced by the extracts derived from the different samples. Each extract was tested in 3 concentrations: (i) undiluted (150 µl), (ii) 1:2 diluted with medium (50 + 100 µl) and (iii) 1:14 diluted (10 + 140 µl). Cell culture medium without extraction was used as the negative control. A toxic PVC-Film (Rehau GmbH, Germany) extracted in the same manner as the samples was used as positive control. After additional 24 h of culture, cytotoxicity was assayed by XTT-Test (cell proliferation Kit, Roche Diagnostics GmbH, Mannheim, Germany).

The assay is based on the cleavage of the yellow tetrazolium salt XTT (sodium 3'-[1-(phenylaminocarbonyl)-3,4-tetrazolium]-bis(4-methoxy-6-nitro) benzene sulfonic acid hydrate) (Roche Diagnostics GmbH, Mannheim, Germany) to form an orange formazan dye by metabolically active cells. Therefore, this conversion only occurs in viable cells. The formazan dye formed is soluble in

aqueous solutions and is directly quantified using a scanning multiwell spectrophotometer (ELISA reader).

3.5.3 Cell attachment

Cell attachment was assessed by seeding SaOS-2 cells with a density of 2.0×10^4 cells/cm^2 for 1 hour and for 2 hours on the specimens. After 1 and 2 hours, respectively, the specimens were rinsed with phosphate-buffered saline (PBS Dulbecco's, Scotland, UK) without magnesium and calcium. They were fixed with 2% paraformaldehyde in PBS for 15 minutes at room temperature, immersed in 1% Triton X-100 in PBS for 5 minutes, and finally incubated with 5% goat serum at room temperature. Vinculin, a protein related to focal contacts, was stained with mouse anti-human-vinculin (Sigma-Aldrich Chemie GmbH, Steinheim, Germany) acting as the primary antibody, and TRITC (tetramethylrhodamine isothiocyanate) conjugated anti-mouse-IgG (Sigma-Aldrich Chemie GmbH, Steinheim, Germany) acting as the secondary antibody. Fixed cells were incubated with FITC-conjugated phalloidin to stain actin filaments. After the fluorescent staining, the specimens were mounted with fluorescence protection mounting medium (Polyvinyl alcohol mounting medium with DABCO; Fluka Chemie GmbH, Buchs, Switzerland) and evaluated in an epifluorescent microscope (Nikon-OPTIPHOT-2, Nikon Co., Japan). The percentage of cells attached on the specimens was calculated using the number of cells on G-1 for 1-hour cell culturing as a reference (100%).

3.5.4 Cell spreading

Cell spreading was assessed by microscopic examination of the specimens after culturing for 1 and 2 hours. Focal contacts and cytoskeleton were examined and documented using fluorescence microscopy (Nikon E950 digital Camera, Nikon Co., Japan). For electron microscopy, specimens were fixed in 2% Glutaraldehyde for 16 hours and dehydrated by passing through a series of alcohols before they were dried in a E3000 (Plano GmbH, Wetzlar, Gemany) Critical Point Drier. The specimens were finally mounted on aluminium stubs

(Plano GmbH, Wetzlar, Gemany) and coated with a thin layer of Au-Pd to examine the cell morphology using a SEM.

As shown in Fig. 2, all attached cells were divided into a) not spread: cells were still spherical in appearance, protrusions or lamellipodia were not yet produced; b) and c) partially spread: at this stage, cells began to spread laterally at one or more sides, but the extensions of plasma membrane were not completely confluent; d) fully spread:
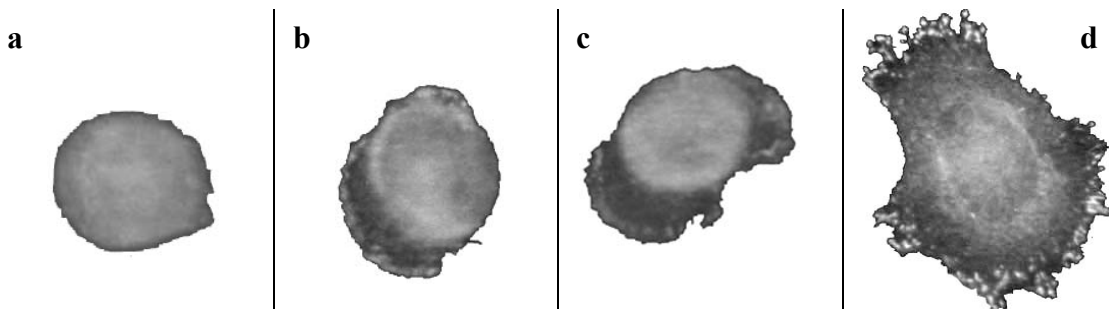

Figure 2 All attached cells were divided into a) not spread: cells were still spherical in appearance, protrusions or lamellipodia were not yet produced; b) and c) partially spread: at this stage, cells began to spread laterally at one or more sides, but the extensions of plasma membrane were not completely confluent; d) fully spread: extension of plasma membrane to all sides, combined with distinctly larger surface area than in stages a to c and obvious flattening of the cell, was observed. All the pictures of cells in this figure were from the present experiment

extension of plasma membrane to all sides, combined with distinctly larger surface area than in stages a to c and obvious flattening of the cell, was observed. The number of total attached cells and percentage of fully spread cells among attached cells were calculated from 5 different random areas (0.8 × 0.8 mm) of each specimen. The mean number of attached cells on the surfaces of the control(cp Ti, G-1) for 1h cell culture was set as 100%, and the data of the other groups were compared with it. Focal contacts sites and cytoskeleton were examined by a Nikon E950 digital Camera (Nikon Co., Japan) under fluorescence microscopy.

3.5.5 Cell proliferation

Each group of specimens used for cell proliferation tests was divided into 3 subgroups and measured after cell culturing for 1, 2 and 4 days, respectively. SaOS-2 cells were cultured on specimen surfaces with the initial cell density of 2.0×10^4 cells/cm^2 in 6-well culture plates. At every harvest time point, cells were detached from specimen surfaces by incubation with Trypsin/EDTA (0.5g/L Trypsin and 0.2g/L EDTA, GIBCO, Scotland, UK) for 5 min at 37ºC, and each specimen was washed with PBS without magnesium and calcium. According to our preliminary tests, the procedure was repeated one more time to confirm no residual cells on surfaces of specimens after this releasing procedure. Released cells were counted with a hemocytometer, and on every specimen counting was repeated three times.

3.5.6 Alkaline phosphatase activity

After cell proliferation test, the cells were collected by centrifugation with 1100 rpm at room temperature for 3 min. The cell pellets were lysed in 400 µl 0.5% Triton, and alkaline phosphatase (ALP) activity was measured using p-nitrophenylphosphate (Sigma Diagnostics, Inc, St. Louis, USA) as substrate. A standard solution from p-nitrophenol (Sigma Diagnostics, Inc, ST. Louis, USA) reacted with 0.1 N NaOH was diluted into a series of standard concentrations with distilled water (Ampuwa, Fresenius Kabi Deutschland GmbH, Bad Homburg, Germany) as references for measurement. Absorbance was measured using an ELISA reader with the wavelength of 405 nm. The value of ALP activity was normalized by the total cell number obtained from proliferation tests, and ALP activity was defined as nMol/min/10^4 cells.

3.5.7 Statistical analysis

All data were analyzed by the JMP Version 5.01 statistical analysis program (SAS Institute Inc., Cary, NC). Significant differences between all the groups and the control were determined using Dunnett's test, which guards against the high alpha size (type I) error rate across the hypothesis tests. The Tukey-Kramer HSD (Honestly Significant Difference) test was used to perform multiple

comparisons between the groups anodized. The Tukey-Kramer HSD test provides a conservative calculation of statistical significance in the analysis of intergroup comparisons, which minimizes the risk of type I error by increasing the quantile multiplied into the standard error values to create the least significant difference. Unless otherwise indicated, all data presented were mean ± S.D. and the significance level of 0.05 (*p) was accepted.

4 Results

4.1 Surface characterization of anodic oxides of titanium

4.1.1 Topography of surface oxides

Figure 3 shows the morphology of pure titanium (control) and anodized titanium surfaces. The control surface had shallow parallel grooves oriented along the polishing direction. The surfaces G-2 and G-5 displayed island-shape films. The increase of the anodising voltage resulted in the gradual formation and development of the anodic oxide film, i.e. from islands to the whole surface, with more and larger irregular micro-pores generated by sparking during anodic oxidation. The grooves produced by polishing were removed gradually as the voltage rose. The detailed studies on topography of anodised surfaces with the applied voltage are investigated in the previous work [145, 146]. The pore geometry (up to ca. 0.5 µm for G-4 in diameter) in electrolyte No. 1 was distinctly smaller than that (up to 2 µm for G-8) in electrolyte No. 2.

As shown in Fig. 4, statistical analyses indicate a significant influence of the anodizing voltage used on surface roughness (Ra) in both electrolyte solutions tested. Significant differences are seen in electrolyte 1 between G-2 and G-3, and G-2 and G-4, respectively, and in electrolyte 2 between G-5, G-6, G-7, and G-8. Therefore, the Ra value of surface roughness on anodic oxides formed in electrolyte No. 1 decreased with an increase in anodising voltage; while in electrolyte No. 2, Ra values became higher with increasing voltage. Statistical significant difference was shown in roughness between anodised surfaces and the control surface, and additionally, there was difference between anodised surfaces except between G-3 and G-4. However, all the Ra values were in the range of 0.1-0.5 µm, which is similar to that of the machined surfaces [2, 85]. Thus, anodic oxidation can increase the surface roughness but only to a limited extent.
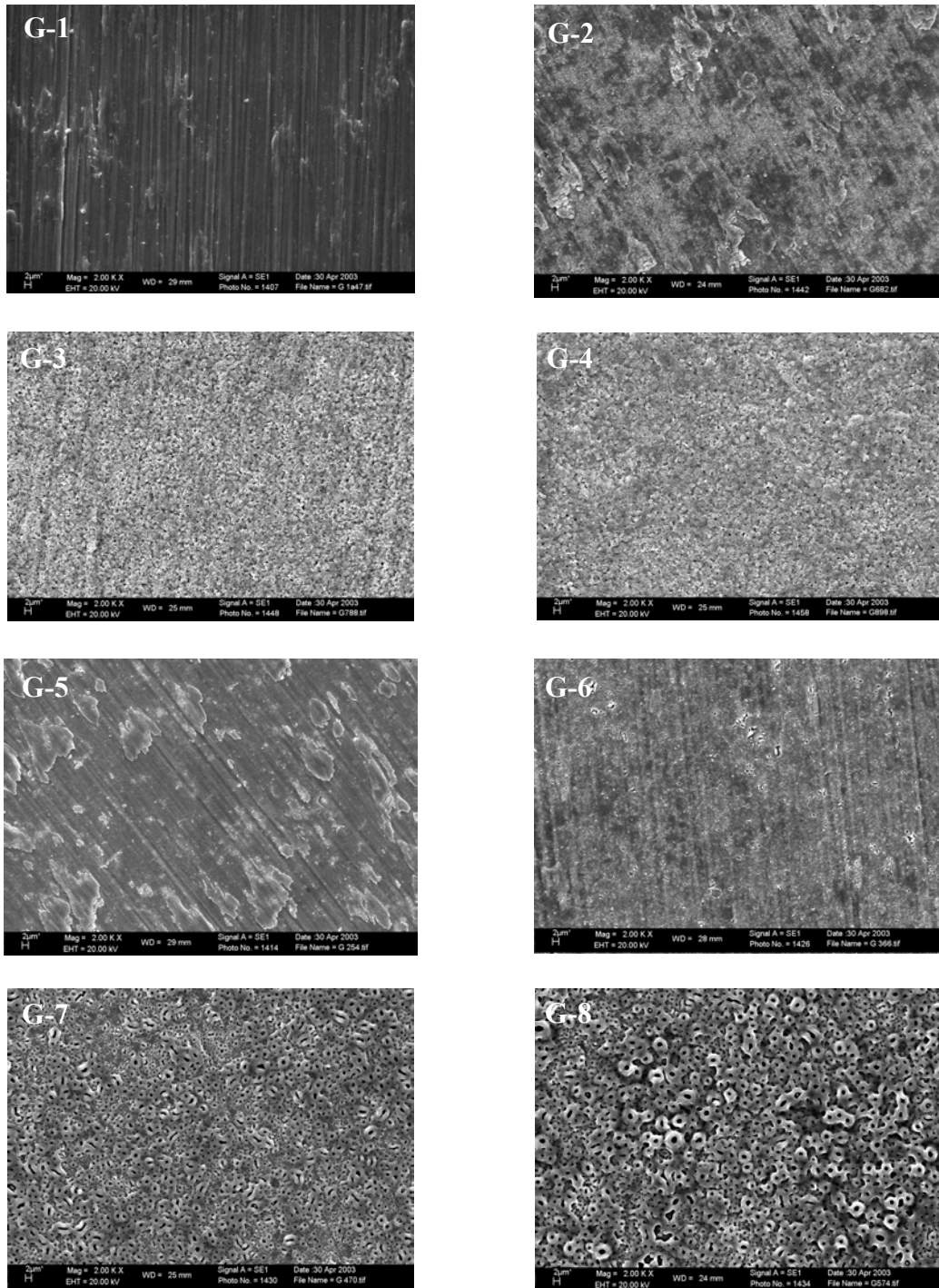
Figure 3. Morphology of the different surfaces of titanium, anodizing conditions: 70 A/m^2, (G-1) pretreated; (G-2) at 200V in 0.2 M H$_3$PO$_4$; (G-3) at 200V in 0.2 M H$_3$PO$_4$;(G-4) at 350V in 0.2 M H$_3$PO$_4$; (G-5) at 140V in 0.03 M Ca-GP and 0.15 M CA;(G-6) at 200V in 0.03 M Ca-GP and 0.15 M CA; (G-7) at 260V in 0.03 M Ca-GP and 0.15 M CA; (G-8) at 300V in 0.03 M Ca-GP and 0.15 M CA

4.1.2 Wettability and surface composition

Contact angle measurements indicate that the values of all contact angles of control (untreated) and anodised surfaces were in there range of 60º to 90º, namely, all the surfaces were hydrophilic surfaces (Fig. 5). At higher anodizing voltages, the corresponding contact angles were higher for the anodic oxides formed in electrolyte No.1 but became lower for those formed in electrolyte No.2. The relationship of contact angles and anodising voltages exhibited a trend exactly opposite to that of surface roughness and voltages, except for G-5.
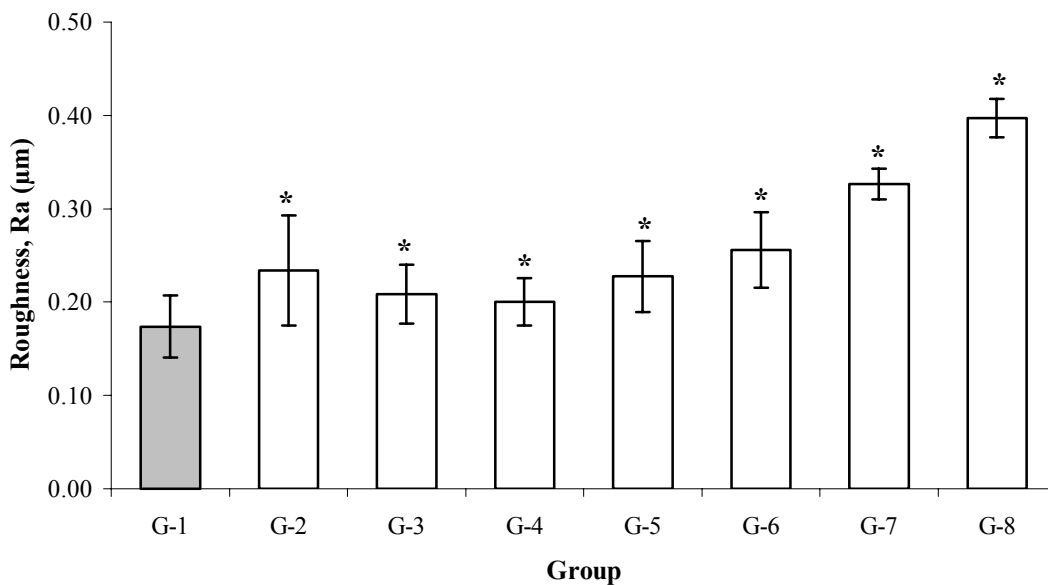
Comparisons for all pairs in the same electrolyte using Tukey-Kramer HSD (Abs(Dif)-LSD)

	G-2	G-3	G-4		G-5	G-6	G-7	G-8
G-2	-0.02411	0.00428[+]	0.01105[+]	G-5	-0.02078	0.00749[+]	0.07818[+]	0.14853[+]
G-3	0.00428[+]	-0.02411	-0.01734	G-6	0.00749[+]	-0.02078	0.04991[+]	0.12025[+]
G-4	0.01105[+]	-0.01734	-0.02411	G-7	0.07818[+]	0.04991[+]	-0.02078	0.04956[+]
				G-8	0.14853[+]	0.12025[+]	0.04956[+]	-0.02078

[+]Positive values show pairs of means that are significantly different (Alpha = 0.05).

Figure 4. Roughness, Ra, of the anodized surfaces of titanium, G-1 as a control, *p <0.05
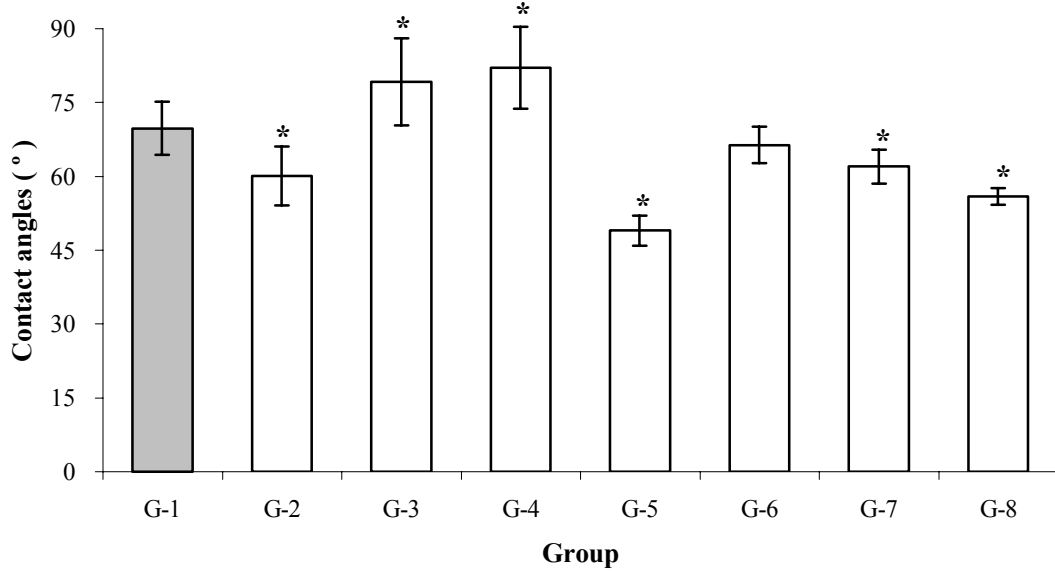
Comparisons for all pairs in the same electrolyte using Tukey-Kramer HSD (Abs(Dif)-LSD)

	G-2	G-3	G-4		G-5	G-6	G-7	G-8
G-2	-8.674	10.496[+]	13.316[+]	G-5	-3.707	13.663[+]	9.323[+]	3.243[+]
G-3	10.496[+]	-8.674	-5.854	G-6	13.663[+]	-3.707	0.633[+]	6.713[+]
G-4	13.316[+]	-5.854	-8.674	G-7	9.323[+]	0.633[+]	-3.707	2.373[+]
				G-8	3.243[+]	6.713[+]	2.373[+]	-3.707

[+] Positive values show pairs of means that are significantly different (Alpha = 0.05).

Figure 5 Wettability of the anodized surfaces of titanium, G-1 as a control, *p <0.05

XPS analyses of the prepared groups indicate that the P content of the anodic oxides (about 10 at.%) was determined by phosphate concentration in electrolyte No. 1, irrespective of anodising voltage; while in the electrolyte No. 2, Ca content (1-6 at.%) of the anodic oxides significantly increased with an increase in anodising voltage and P content (3-6 at.%) was almost not affected by voltage except for at 140 V (Table 2). Ca/P ratios in anodic oxides had the trend to increase with increasing anodising voltage or thickness of oxides in both electrolytes. The contaminants of carbon (20-30 at.%) (C), silicon (Si) nitrogen (N) and partially oxygen (O) originate from air, the polishing and sterilization process and/or electrolytes. The chemical composition of G-1 (control), as provided by the manufacturer, consists of 0.007% N, 0.014% C, 0.002% H, 0.06% Fe, 0.150% O, residuals <0.3% in total and Ti of balance.

Table 2 Chemical composition of anodic oxides of titanium by XPS (at.%)

Group	Ti	O	C	P	Ca	N	Si	Other[*]	Ca/P
2	10	56	18	10		1	<0.1	5	
3	7	53	23	10		2	1	4	
4	7	47	31	11		2	<0.1	< 2	
5	15	55	24	3	<1	2	<0.1	1	<0.33
6	14	54	23	5	2	<1	<0.1	2	0.40
7	13	55	20	6	4	<0.1	<0.1	< 2	0.67
8	12	54	20	6	6	<0.1	<0.1	< 2	1.00

[*]not clearly identified

The Ti 2p, O 1s, C 1s, P 2p and Ca 2p XPS spectra of titanium anodic oxides formed in either electrolyte are shown in Figure 6. The spectrometer was calibrated by using Au $4f_{7/2}$ (84.0 eV) signal. Using the C1s main peak a charge shift of + 1.1 eV (G-4) and + 0.9 eV (G-8) has been determined. The Ti 2p peaks of anodic oxides of G-4 and G-8 were well fitted to those of Ti 2p in TiO_2 and Ti was identified to be in the form of TiO_2. In the O 1s spectra, three peaks for either G-4 or G-7 were fitted at binding energies 530.1 ± 0.2, 531.3 and 532.8 ± 0.1 eV, respectively, after correction of charge shift. The peak located at 531.3 eV corresponded to O 1s in PO_4^{3-} [43], A second peak at 1.3 eV lower binding energy (ca. 530.1 eV) was assigned to O 1s of TiO_2 since its binding

energy was shown in the range from 529.9 to 530.9 eV [24]. The third peak at ca. 532.8 ± 0.1 was attributed to the contributions from the following probable
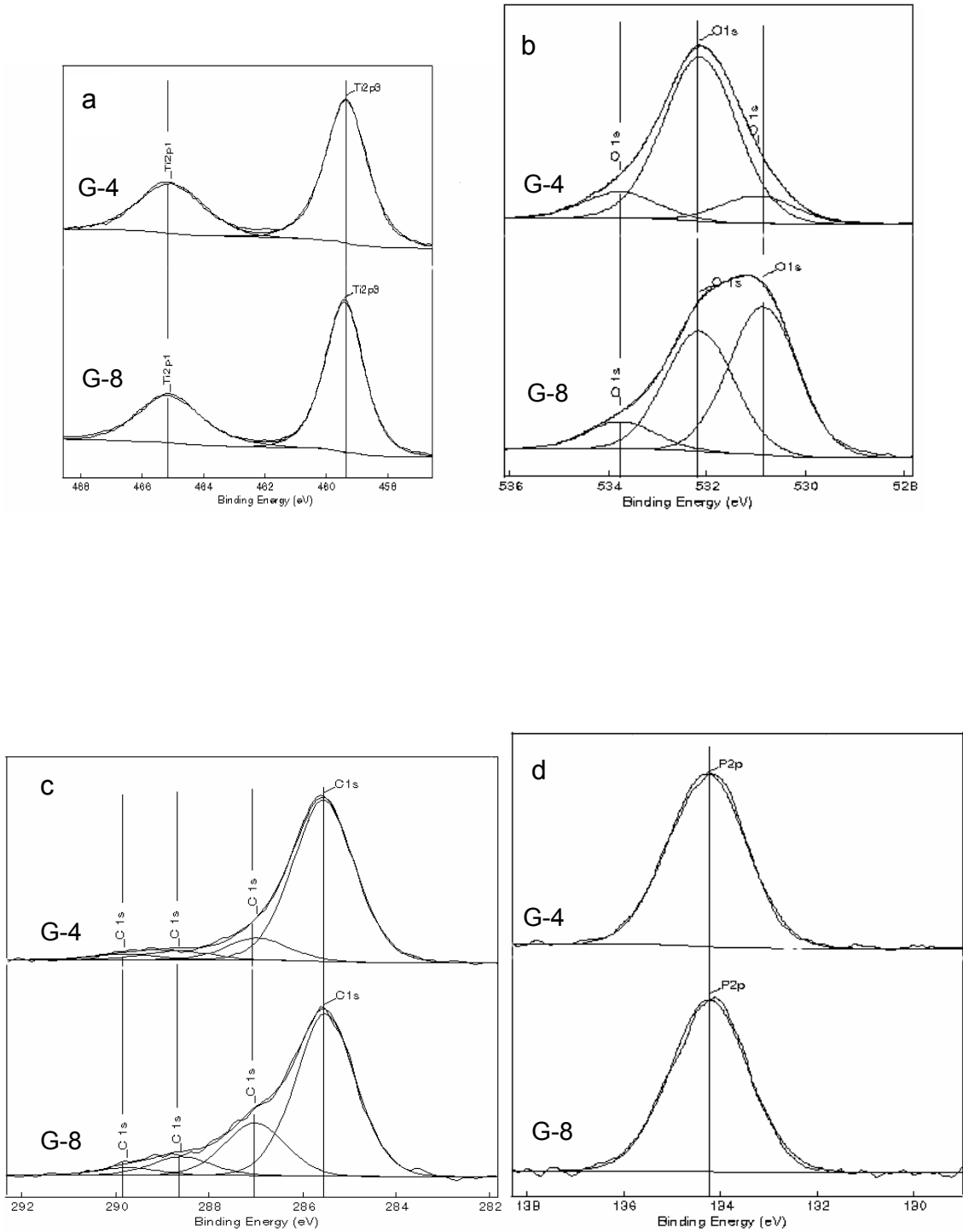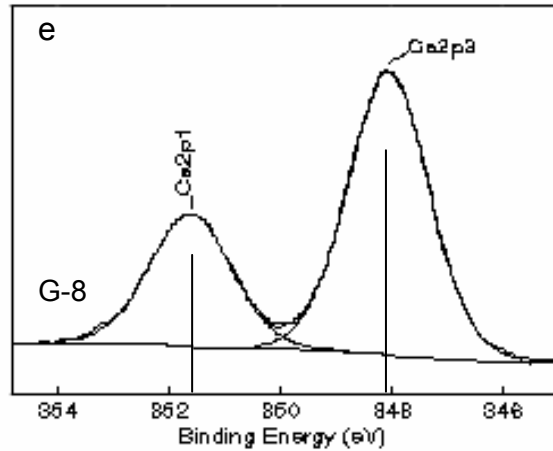
Figure 6 High-resoultion XPS spectra of anodized surfaces of titanium (a) Ti 2p;
(b) O 1s; (c) C 1s; (d) P 2p; (e) Ca 2p

groups, i.e. ether groups C-O or O-C-O [190], HPO_4^{3-} [43], basic hydroxyl [114]
and chemisorbed water [84] , respectively. The third peak of O 1s became
higher in G-8 comparing with that in G-4, and it is ascribed to more ether groups
or hydroxyl groups from electrolyte No.2 than those from electrolyte No.1. From
the C 1s spectra, four peaks were fitted and analysed according to the
literature. The predominant peak (C_0) at 284.6 eV corresponded to organic
carbon (C-H, C-C), and the other three peaks with the binding energy ca.C_0 +
1.5, C_0 + 3.1 , and C_0 + 4.1eV were assigned to C-O, C=O, O-C=O, respectively
[43]. The peak corresponding to C-O of G-8 was remarkably higher than that of
G-4 and the higher peak of C-O in the surface oxide formed in electrolyte No.2
may be related to the C-O bonds of the glycerophosphate of the electrolyte. The
P 2p peaks in G-4 and G-8 were well fitted at 133.3 eV and 133.4 eV, and
assigned to phosphorus in PO_4^{3-} (at 133.4 eV) not HPO_4^{3-} (at 134.4 eV) [43].
The Ca $2p_{3/2}$ peaks in G-4 with binding energy $2p_{3/2}$ at 347.1 eV and $2p_{1/2}$ at
350.9 eV corresponded to calcium in calcium phosphate [32] and no calcium
hydroxide or calcium linked to carbonate groups was demonstrated since the
corresponding Ca $2p_{3/2}$ binding energy of either of them should be much lower

(ca. 345.7 eV) [43]. Besides, no information of calcium was collected in the surface oxides of G-8 due to no calcium source.

4.2 Ultraviolet (UV) treatment of anodic oxides of titanium

As shown in Fig. 7, before UV irradiation, static contact angles of anodic oxides on titanium increased at first till at about 220 V and then decreased with an increase in anodising voltage. The hydrophilicity of anodised surfaces was demonstrated to be higher than that of cp titanium except for surfaces anodised at 220 V and 240 V, which were comparable to or slightly higher than cp titanium in contact angle.
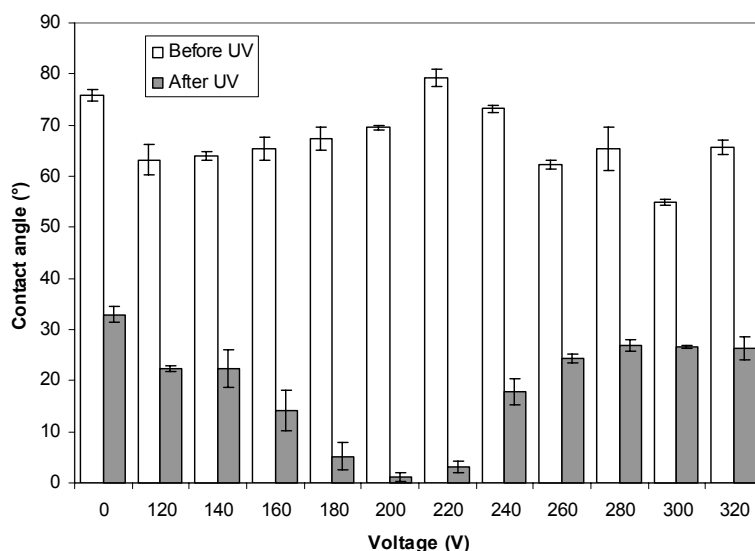
Figure 7 Hydrophilicity of anodised surfaces of cp Ti before and after UV irradiation

The morphology of anodic oxides on the surface of cp titanium varied from planar with polished grooves to porous structures, which are dependent on anodising voltages (Figure 8). During anodic oxidation, noticeable sparking began to occur on the surface at about 180 V, thereby forming small amount of irregular pores inhomogeneously in the surface oxides. As anodising voltage was raised, micro-pores of anodic oxides became more in number at first and then fewer in number but larger in size. The surface oxides at 220 V displayed

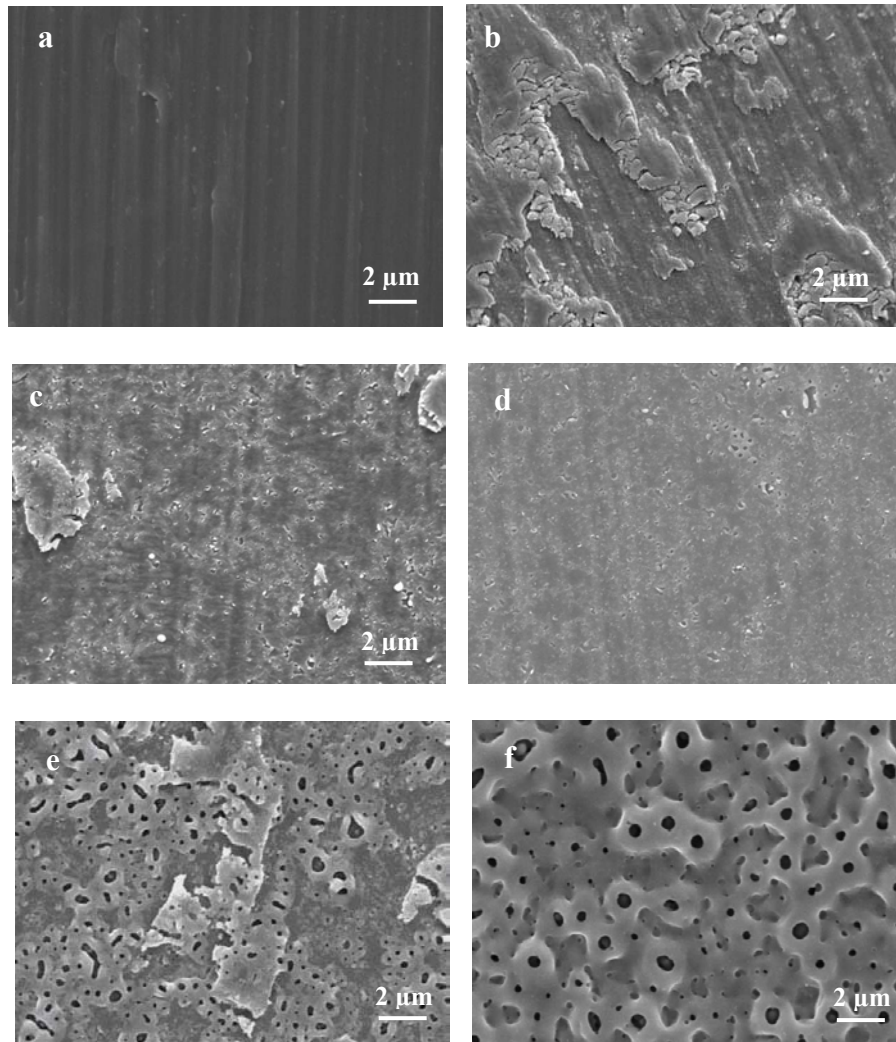the highest density of pores, which would be further confirmed by the following surface texture parameters.

Figure 8 Morphology of surface oxides of titanium (a) 0V, (b) 140V, (c) 180V, (d) 200 V, (e) 220V, (f) 300V

For porous surfaces, air trapped in pores would produce a possible barrier for a water droplet to spread on the border of pores. This effect, which enhances hydrophobicity, may be similar to that found on textured surfaces or microetched titanium surfaces. On the other hand, their surface composition was altered by the entrance of small amount of Ca and P, the amount of which

was increased in surface oxides formed at higher anodising voltage. As both Ca and P are polar solutes in water, their incorporation produces a polar surface, which assists water to wet the surface. The contact angles of anodised surfaces were suggested to be affected mostly by surface topography and composition, thereby showing the initial increase and then decrease as anodising voltage increased. The peak in contact angle vs. anodizing voltage is on account of speciality of its surface structure at 220 V, e.g. the highest density of pores.

After UV irradiation, as a droplet was applied for measurement of wettability, an attracting force could be noticed acting from the specimen surface on the pendant water droplet to pull it drip down as it approached the irradiated surface. As shown in Fig. 7, the UV induced hydrophilization occurred to all the oxides on titanium. However, alteration of contact angles induced by UV irradiation was distinctly different. The minimum contact angle after UV treatment was positioned around 200 to 220 V, which exactly corresponds to where the peak of contact angles positioned before UV irradiation, or the special surface texture with the highest pore density in the oxides.

4.3 Structure of nanocrystalline HA

The XRD patterns of the prepared HA particles show that all the peaks of nanocrystalline HA became significantly higher as aging temperature increased (Fig.9a), while the elongation of aging time did not demonstrate any influence on the intensity of the peaks in XRD patterns (Fig.9b). By semi-quantitative analysis, the average crystalline size of nano HA was in the range of 20 to 50 nm from the full width at half maximum of the reflections and demonstrated the tendency to increase as aging temperature increased and. As shown in Fig.10a, HA nanoparticles were revealed to be in the shape of ellipsoid, that is, anisometric particle growth, and the average size of crystals in the long axis was estimated to be in the range of 20-30 nm, which agrees with the calculation by Scherre equation from XRD patterns. Electron diffraction rings (Fig.10b), according to D-spacing values, were identified to be (002), (112) and (310) or (221), respectively.

Furthermore, after annealed at the temperature from 300 to 900 °C, peaks of XRD patterns of nano HA became higher as annealing temperature was enhanced (Fig.11). However, no new peak appeared.
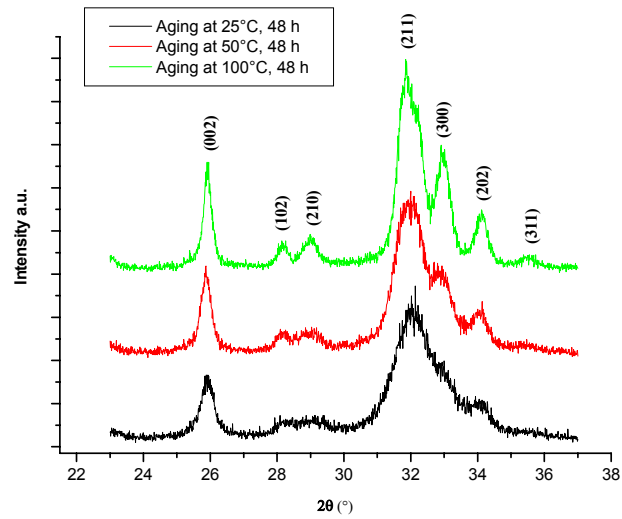
(a)
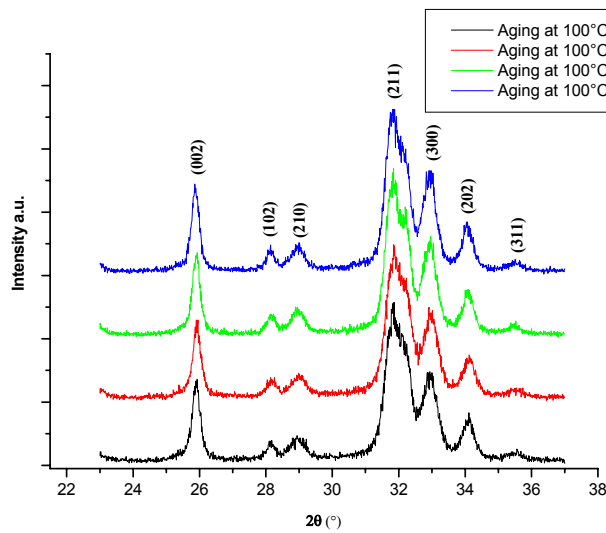
(b)

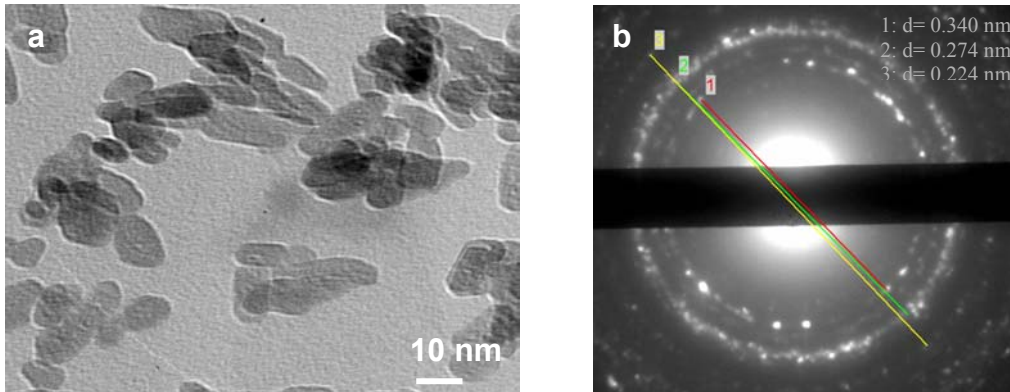Figure 9 XRD patterns of nano HA via aging temperature (a) and time (b)

Figure 10 Structure of nano HA synthesized aging at 100 °C for 48 hours
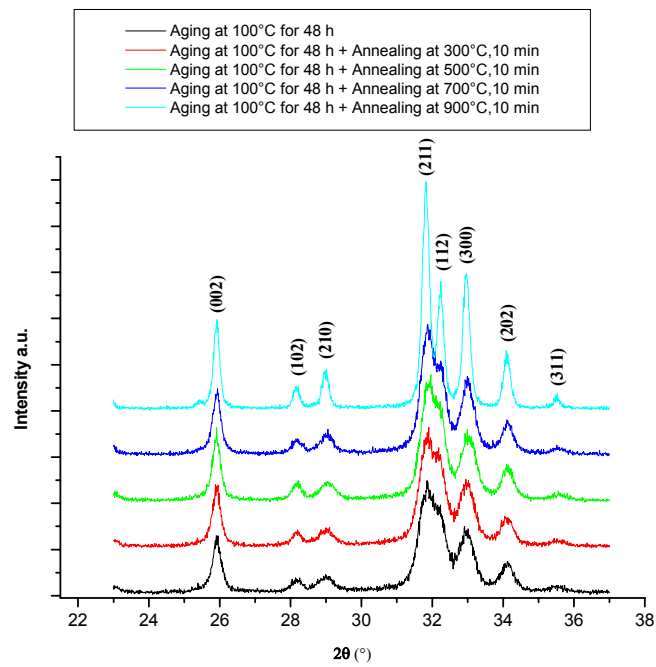

Figure 11 Structures of nano HA annealed at different temperatures

4.4 Surface characteristics of deposited nano HA or nano HA/collagen surfaces

Figure 12 shows contact angles of different surfaces with deposited HA or HA/collagen on titanium surfaces. A significant statistical difference was exhibited for the deposited substrate surfaces in contact angles, that is, θ (G-2) > θ (G-1) > θ (G-3). After depositing nano HA, the corresponding surfaces had remarkably reduced contact angles. Interestingly, the decrease of contact angles was related to data of contact angles of the substrate surfaces, i.e. the surfaces before deposition of nano HA. The higher the contact angle of the substrate surface is, the lower is the contact angle value of the deposited nano-HA surface. There was no significant statistical difference in contact angle between the surfaces deposited with nano HA and nano HA/collagen. The decrease of contact angles by nano HA deposition is ascribed to high surface energy of nano HA particles. In contrast, collagen involvement did not affect the surface wettability of deposited nano HA on different titanium surfaces except for G-7-HC.

The roughness of the different surfaces was evaluated with roughness parameters, such as Ra, Rp, Rmax and Rz (Fig.13). From statistical analyses, surface roughness was decreased by depositing nano HA, while the surface roughness had no remarkable difference for nano HA/collagen coatings compared to nano HA coatings. Since nano HA coatings covered the whole substrate surface, all the substrate surfaces displayed lower roughness. Owing to sufficient dissolution of collagen, nano HA/collagen did not change surface roughness of nano HA coatings.
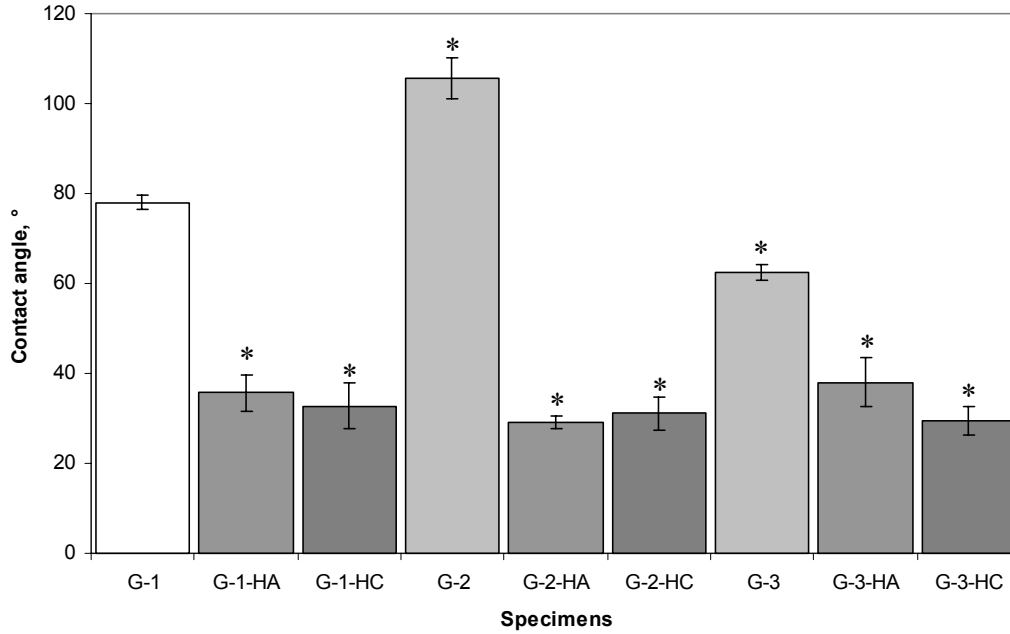
Comparisons for all pairs using Tukey-Kramer HSD

Abs(Dif)-LSD	G-1	G-1-HA	G-1-HC	G-3	G-3-HA	G-3-HC	G-7	G-7-HA	G-7-HC
G-1	-4.839	37.528$^+$	40.428$^+$	22.736$^+$	44.020$^+$	42.170$^+$	10.786$^+$	35.245$^+$	43.611$^+$
G-1-HA	37.528$^+$	-4.839	-1.939	65.103$^+$	1.653$^+$	-0.197	21.903$^+$	-2.555	1.245$^+$
G-1-HC	40.428$^+$	-1.939	-4.839	68.003$^+$	-1.247	-3.097	24.803$^+$	0.345$^+$	-1.655
G-3	22.736$^+$	65.103$^+$	68.003$^+$	-4.839	71.595$^+$	69.745$^+$	38.361$^+$	62.820$^+$	71.186$^+$
G-3-HA	44.020$^+$	1.653$^+$	-1.247	71.595$^+$	-4.839	-2.989	28.395$^+$	3.936$^+$	-4.430
G-3-HC	42.170$^+$	-0.197	-3.097	69.745$^+$	-2.989	-4.839	26.545$^+$	2.086$^+$	-3.397
G-7	10.786$^+$	21.903$^+$	24.803$^+$	38.361$^+$	28.395$^+$	26.545$^+$	-4.839	19.620$^+$	27.986$^+$
G-7-HA	35.245$^+$	-2.555	0.345$^+$	62.820$^+$	3.936$^+$	2.086$^+$	19.620$^+$	-4.839	3.528$^+$
G-7-HC	43.611$^+$	1.245$^+$	-1.655	71.186$^+$	-4.430	-3.397	27.986$^+$	3.528$^+$	-4.839

$^+$Positive values show pairs of means that are significantly different (Alpha = 0.05).

Figure 12 Wettability of nano HA and nano HA/collagen on titanium surfaces
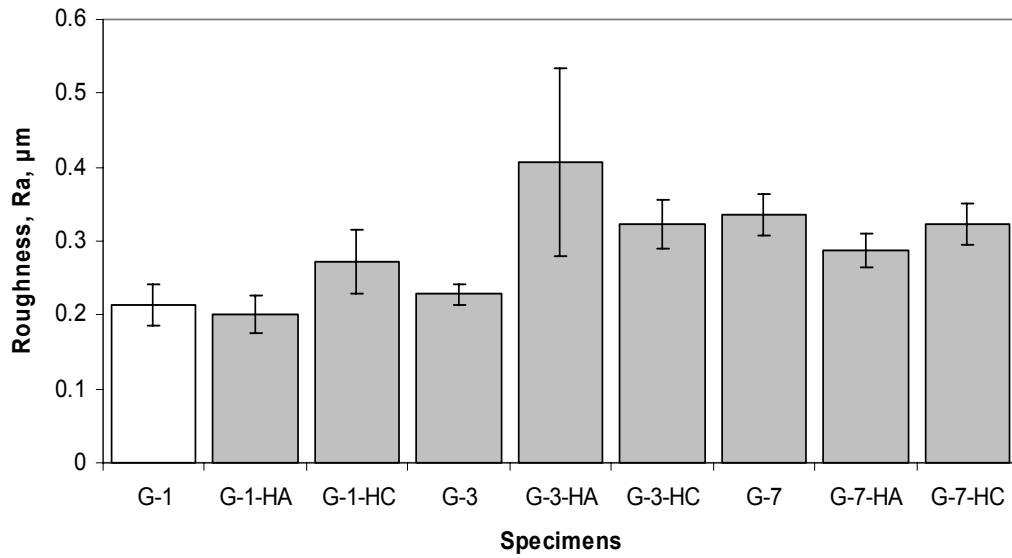
(a)
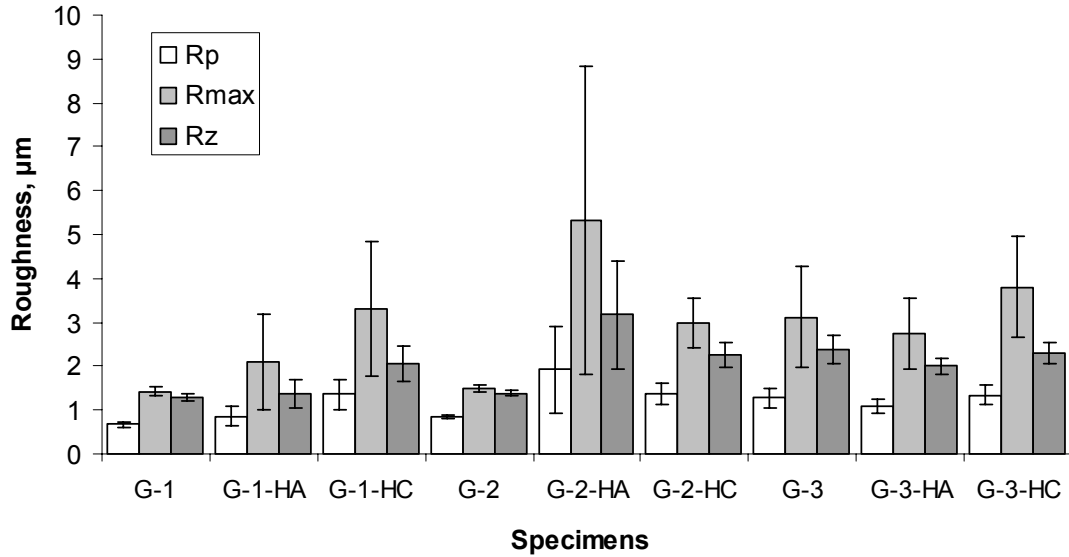
(b)

Figure 13   Roughness (Ra, (a); Rp, Rmax, Rz, (b)) of nano HA and nano HA/collagen coatings on titanium surfaces

4.5 Biological responses to anodic oxides, nano HA and nano HA/ collagen coating on titanium

4.5.1 Cell adhesion on anodic oxides of titanium

(a) Cytotoxicity

Figure 13 shows the cytotoxicity of extracts from all the specimens of anodized surfaces, expressed as decrease in metabolic activity of cells. No statistical significant difference in metabolic activity was shown between negative control and all the groups, while the concentration-dependent decrease in metabolic activity of the positive control (PVC) demonstrates the sensitivity of the assay. Consequently, anodized titanium surfaces with different contents of P or Ca and P do not reduce the viability and metabolism of osteoblasts.
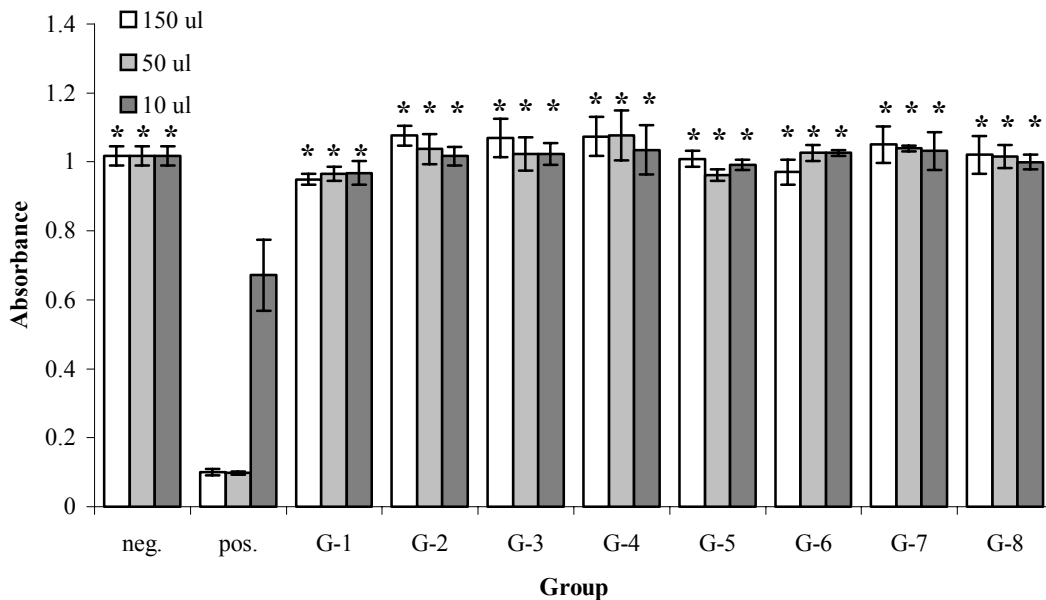

Figure 14 Cytotoxicity of extracts of cp Ti and anodized titanium determined with SaOS-2 osteoblasts at different extract dilutions by XTT-assay. Pure cell culture medium was used as a negative control and an extract from toxic PVC as a positive control, There was significant statistical difference between the positive control and all the groups and no statistical difference between the negative control and all the groups, *p <0.05

(b) Cell attachment and spreading

At 1 and 2 hours, statistical analysis shows that the number of cells attached on nearly all the anodized oxides was apparently higher than on the surface of the control (Fig. 15), that is, initial cell attachment was enhanced by anodic oxidation. The surfaces formed at higher voltages indicated enhanced cell attachment in either electrolyte.

As indicated in Fig.16, the cell spreading assay demonstrated no statistical significant difference concerning the percentages of fully spread cells between the control and the different anodised surfaces at 1 hour. According to statistical analysis, at 2 hours, attached cells on G-2 and G-8 displayed noticeably fewer fully spread cells than on the control, and G-8 had the lowest spreading percentage.
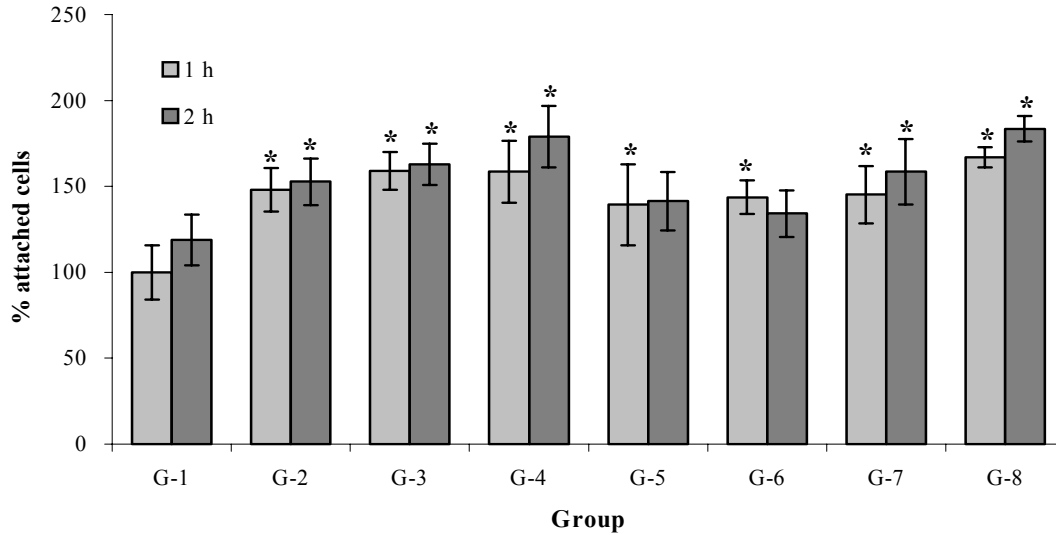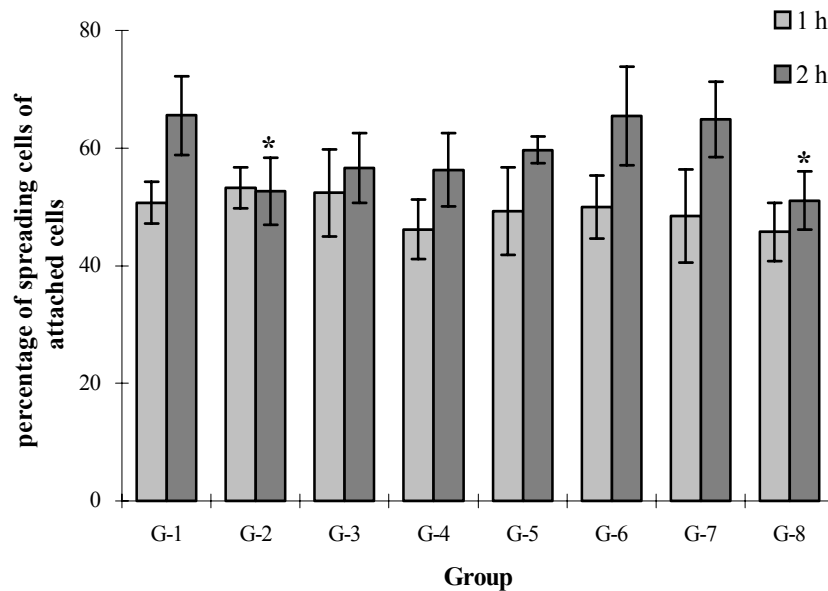
Comparisons for all pairs in the same electrolyte using Tukey-Kramer HSD (Abs(Dif)-LSD) (2 h)

	G-2	G-3	G-4		G-5	G-6	G-7	G-8
G-2	-24.743	-14.499	1.599[+]	G-5	-26.956	-19.638	-9.884	14.994[+]
G-3	-14.499	-24.743	-8.645	G-6	-19.638	-26.956	-2.566	22.312[+]
G-4	1.599[+]	-8.645	-24.743	G-7	-9.884	-2.566	-26.956	-2.078
				G-8	14.994[+]	22.312[+]	-2.078	-26.956

[+] Positive values show pairs of means that are significantly different (Alpha = 0.05).

Figure 15 Percentage of attached cells on anodic oxides normalized by number of attached cells cultured on the surfaces of pretreated Ti for 1h,*p <0.05

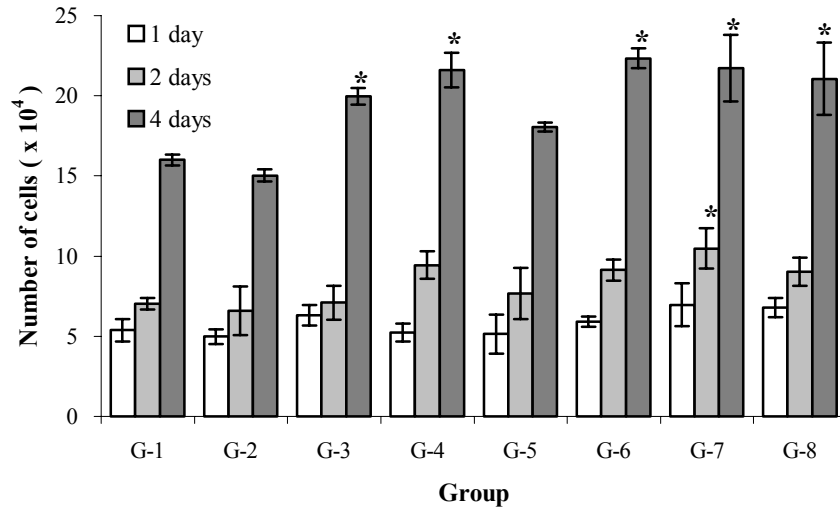Comparisons for all pairs in the same electrolyte using Tukey-Kramer HSD (Abs(Dif)-LSD) (2 h)

	G-2	G-3	G-4			G-5	G-6	G-7	G-8
G-2	-10.055	-6.113	-6.407		G-5	-10.741	-4.979	-5.531	-2.101
G-3	-6.113	-10.055	-9.761		G-6	-4.979	-10.741	-10.189	3.661[+]
G-4	-6.407	-9.761	-10.055		G-7	-5.531	-10.189	-10.741	3.109[+]
					G-8	-2.101	3.661[+]	3.109[+]	-10.741

[+] Positive values show pairs of means that are significantly different (Alpha = 0.05).

Figure 16 Percentage of spread cells of attached cells on the surfaces of pretreated Ti and anodized titanium, *p <0.05

(c) Proliferation and alkaline phosphatase (ALP) activity

As shown in Fig.17, there was no statistical difference between the control and anodized surfaces for cell proliferation after 1 day, and 2 days except G-7. At day 4, higher cell proliferation compared to that on the control was statistically shown on almost all the anodized surfaces except for G-2 and G-5.

Comparisons for all pairs in the same electrolyte using Tukey-Kramer HSD (Abs(Dif)-LSD) (Days 4)

	G-2	G-3	G-4		G-5	G-6	G-7	G-8
G-2	-1.9786	2.7395[+]	4.5914[+]	G-5	-4.0985	0.1815[+]	-0.4285	-1.1018
G-3	2.7395[+]	-2.4233	-0.5938	G-6	0.1815[+]	-4.0985	-3.4885	-2.8152
G-4	4.5914[+]	-0.5938	-1.9786	G-7	-0.4285	-3.4885	-4.0985	-3.4252
				G-8	-1.1018	-2.8152	-3.4252	-4.0985

[+] Positive values show pairs of means that are significantly different (Alpha = 0.05).

Figure 17 Cell proliferation on the different surfaces of titanium. Osteoblasts were seeded at 2.0×10^4 cells/cm^2 onto specimens. The culture medium was renewed every 2 days. After 1, 2 and 4 days, the medium was removed and the cells were washed with PBS, and counted with a hemocytometer. *p <0.05.

No statistical difference of ALP activity was found between the control and anodized surfaces after cell culture for 1 or 2 days (Fig. 18). At day 4, the ALP activity of cells on G-6 was statistically lower than on the control and other anodized surfaces. With the increase of culturing time, the ALP activity

decreased. This can be attributed to the preponderance of the proliferation of cells over the production of ALP activity.
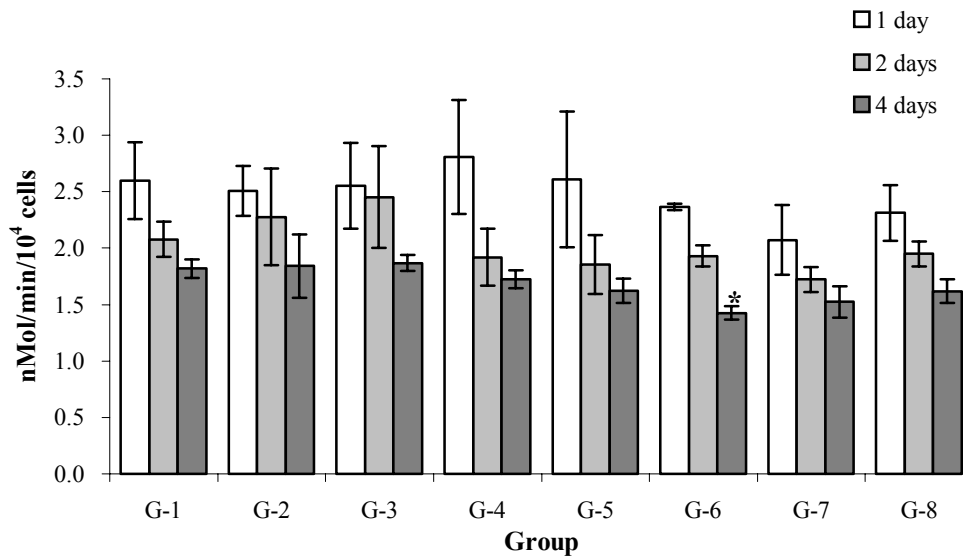

Figure 18   Alkaline phosphatase (ALP) activity of cells on the difference surfaces of titanium for 1, 2 or 4 days. *p <0.05.

(d) Cell reactions to porous surfaces

Fig. 19 shows fully spread cells on various surfaces at 1 and 2 hours. Three kinds of fully spread cell morphologies were shown, that is, a polygonal shape; a polarized shape, i.e. elongated in the opposite directions, mostly occurring in cells on the oxides formed in electrolyte No. 1; and a round one as appeared on the control. At 1 hour, most of fully spread cells on the control were round; while cells adhered on G-2, G-4, G-7 and G-8 became irregular and polygonal. At 2 hours, the morphology of the fully spread cells on the control was not yet changed much and only few cells showed irregular extensions though the number of fully spread cells on the control surface was significantly increased.

After 1 and 2 hours, lots of focal contacts were shown on the control, while cells on anodized surfaces with high voltages such as G-4, G-7 and G-8 developed the fewest number of focal contacts. The formation and development of focal

contacts are probably affected by surface morphology. More irregular pores on these groups may reduce the formation of the observed focal contacts.

As illustrated in Fig.20, after 1 hour of cell culture, the actin cytoskeleton in most of the cells on the surface of the control was not well organised, and lamellipodia supported by the circumferential actin cytoskeleton were formed. Among all the surfaces, the stained lamella were most intensely displayed along the perimeters of the cells on the control and G-5. However, on the surfaces of G-2, G-4, G-7 and G-8 cells were multipolar and their edge was invisible. At 2 hours, the actin cytoskeleton was well organised for the cells on all the surfaces. Thus, the time-dependant organisation of the actin cytoskeleton is influenced by the different anodized surfaces. On the surfaces of the control and G-5 many thick stress fibres, long bundles of assembled actin filaments, crossing the whole cell were viewed, and however, on the surfaces of other groups no apparent stress fibres were observed in cells.
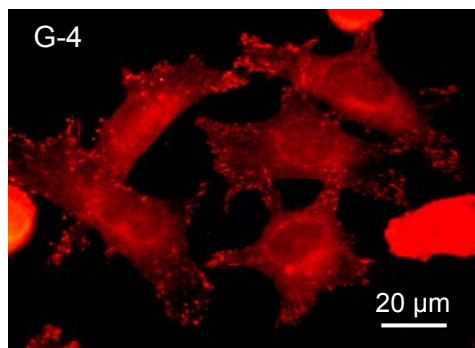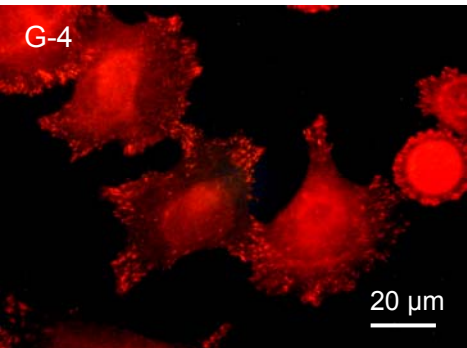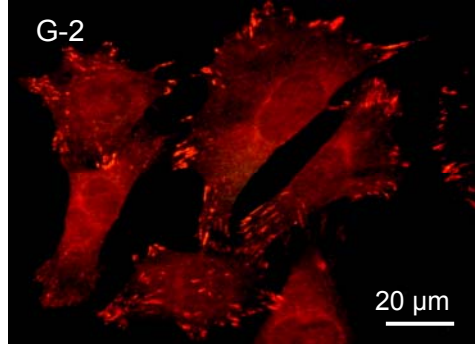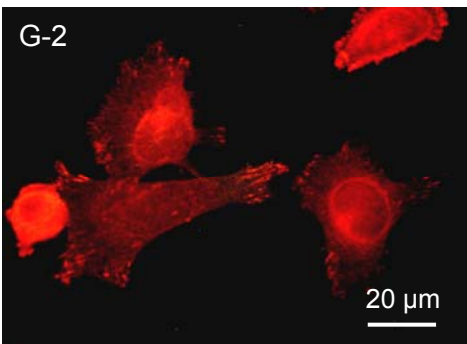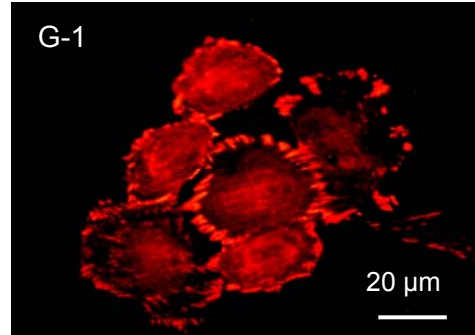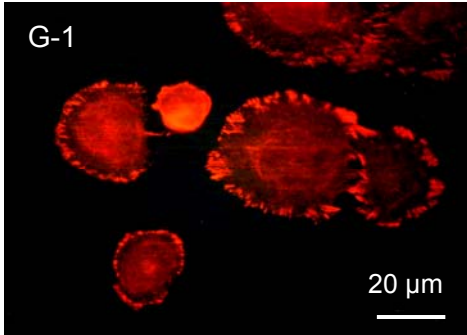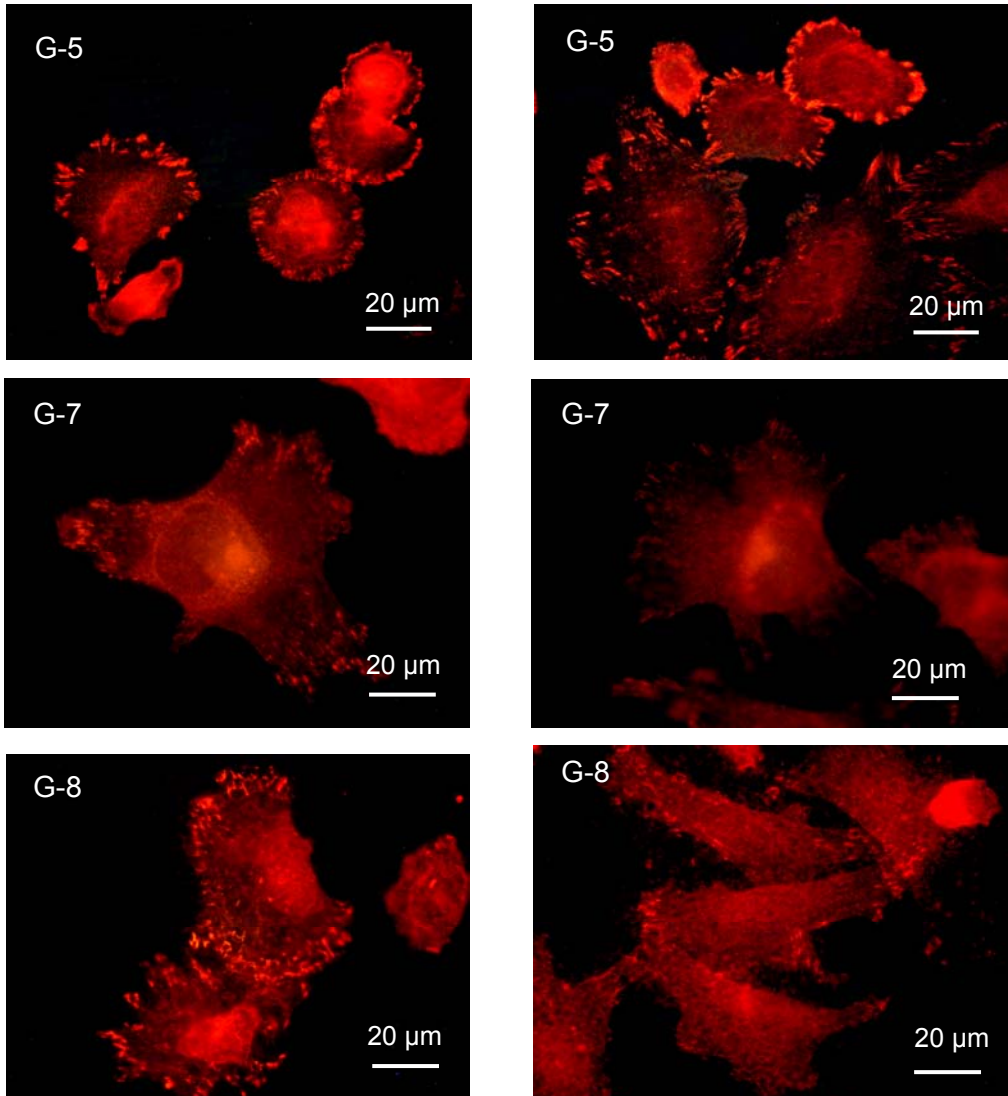
Figure 19 Focal adhesions of cells cultured for 1 and 2 h on the different surfaces of titanium were stained with anti-vinculin: 1h (left); 2h (right)
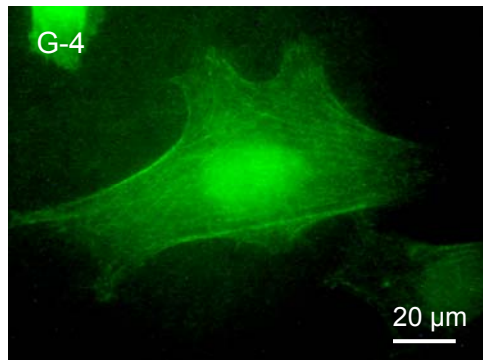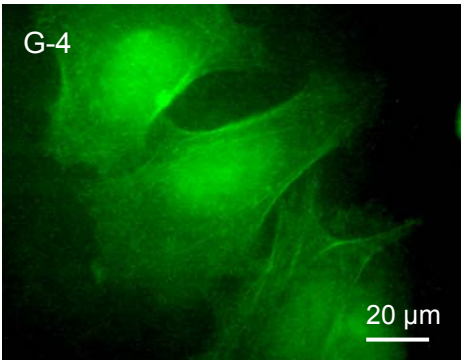
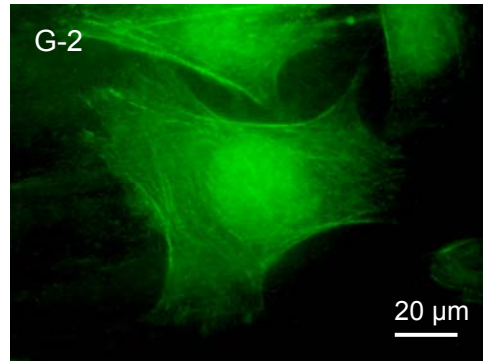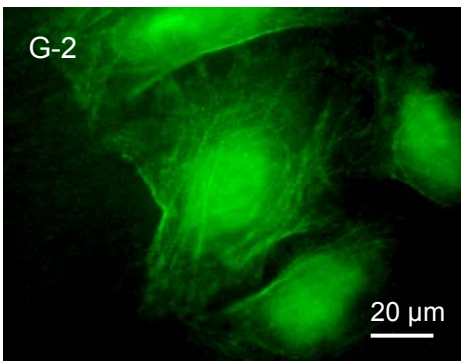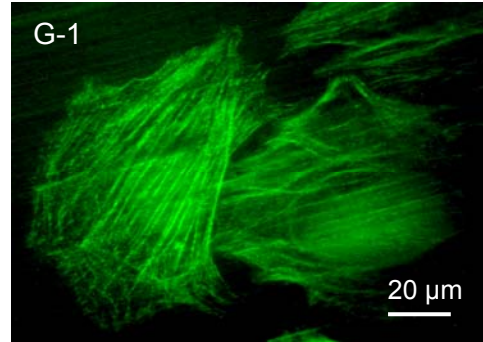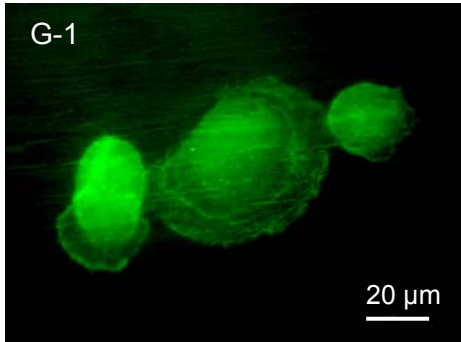Figure 20   Actin cytoskeleton of cells cultured for 1(left) and 2 h (right) on the different surfaces of titanium was stained with phalloidin

Figure 21 shows that after 1 hour, small extensions of the cytoplasmic membrane, i.e. lamella and lamellipodia, were formed on G-1 with some short filopodia around part of the cellular body. In contrast, cells on G-4 and G-8 extended many thin and long filopodia, which attached the cell to the surface. Interestingly, some of the filopodia extending from the cells on G-4 and G-8 entered and connected to certain pores (shown by arrowheads), This phenomenon was found to be independent of the pore size. After culturing for 2 hours, the cells on G-1 displayed complete spreading and intimate adhesion to the underlying surface by adapting the plasma membrane extensions to the change of the substrate topography. However, no discernable filopodia were found; while the cells on G-4 showed a multipolar shape and no intimate adhesion to the underlying substrate, keeping high motility. Also, a significant number of filopodia were viewed around their multipolar edges. The cells on G-8 showed widely spread extension of the plasma membrane, and some lamellipodia and filopodia entered pores as indicated by the arrowheads. However, the cells spread much less than those on G-1 while their nuclei remained ellipsoidal in shape.

4.5.2 Cell responses to the coating of nano HA and nano HA/collagen

After culturing for 1 hour, cells on G-1 displayed a round shape and the most spread among all the groups (Fig. 22). In contrast, cells just attached to the deposited nano HA surfaces, i.e. G-1-HA, did not display any spreading, while cells on the nano HA/collagen surface were in a polarized shape. At 2 hours, cells on G-1were well spread, and well-developed stress fibers were visualized across the whole cells on G-1,while cells on G-1-HA were much less spread, but they developed multipolarly, and cell adhesion and spreading on the nano HA/collagen-coated surface, i.e. G-1-HC, were between G-1 and G-1-. Cell adhesion and spreading on G-7-HA and G-7-HC were similar to those on G-1-HA and G-1-HC. This results from the same coatings, i.e. nano HA and nano HA/collagen.
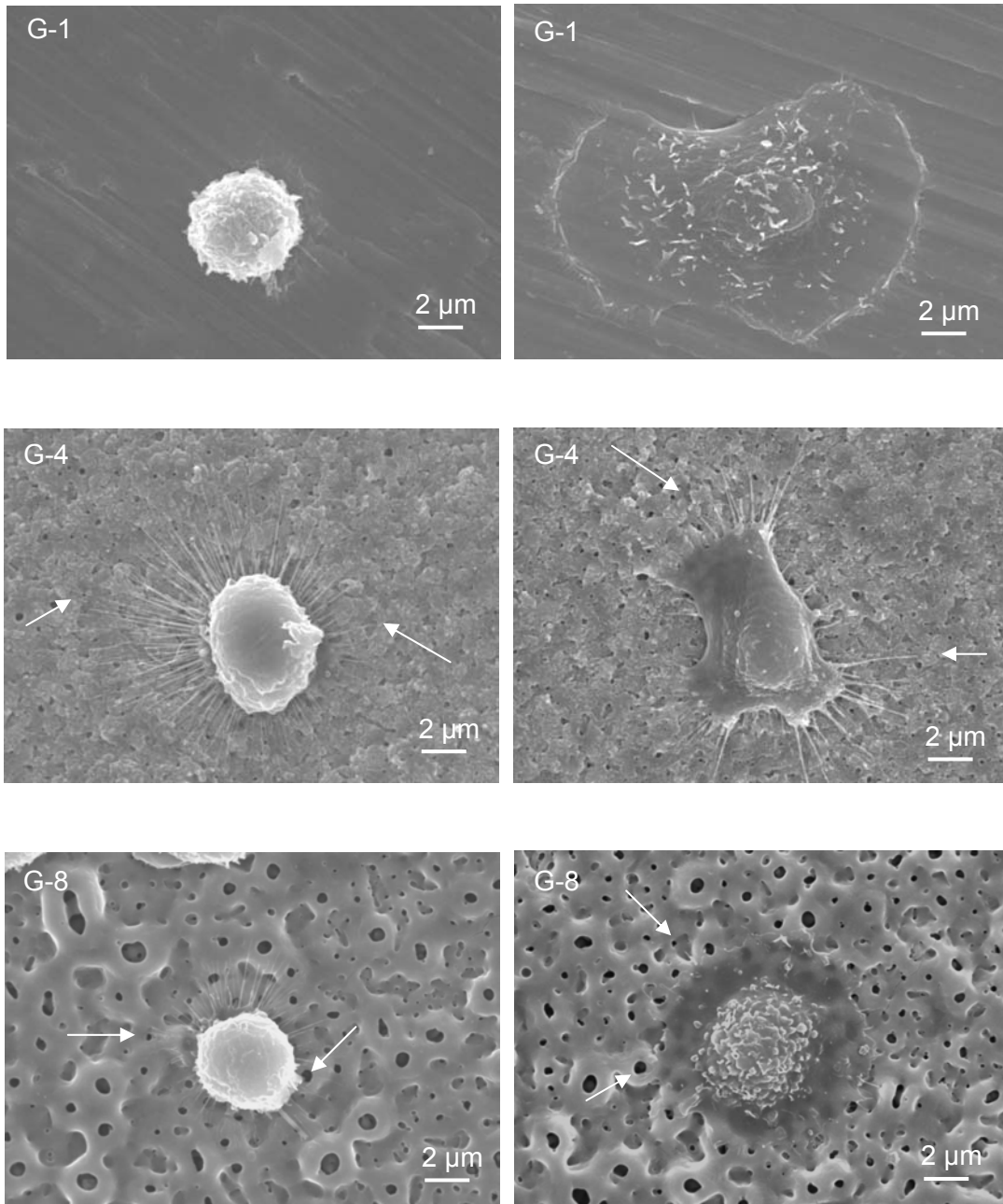
Figure 21 Morphology of cells cultured for 1 h (left) and for 2 h (right) on the different surfaces of titanium G-1, G-3, and G-7

G-1

G-1

25 µm

25 µm

G-1-HA

G-1-HA

25 µm

25 µm
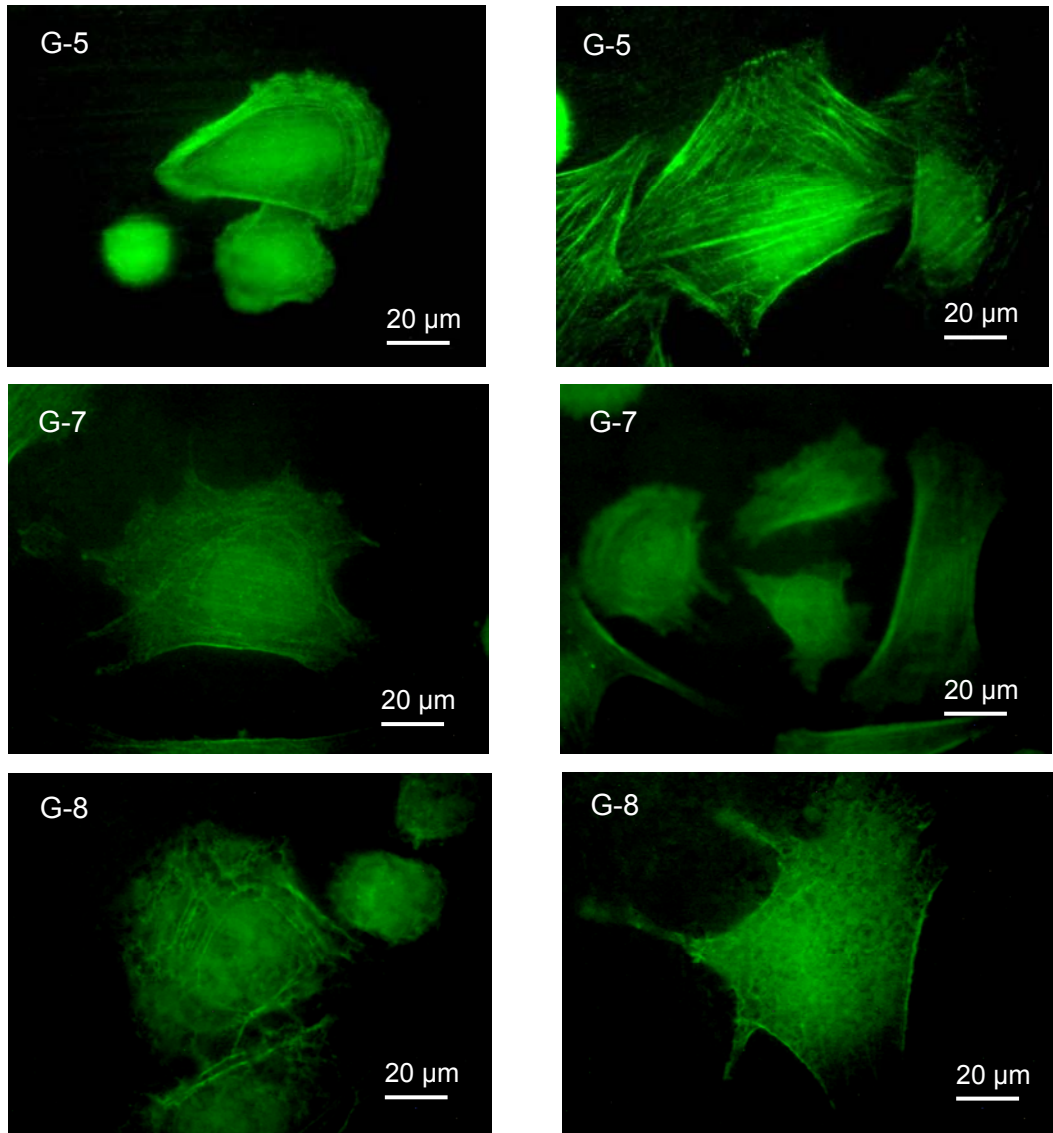
G-1-HC

G-1-HC

25 µm

25 µm

G-7

G-7

25 µm

25 µm
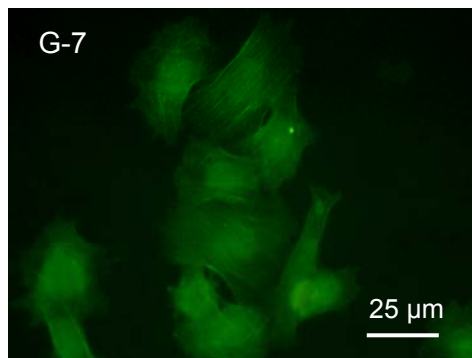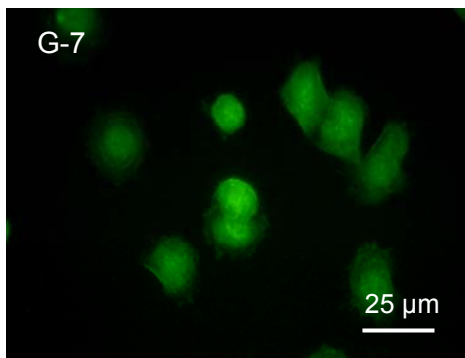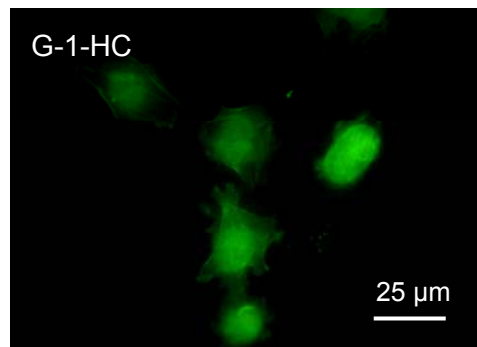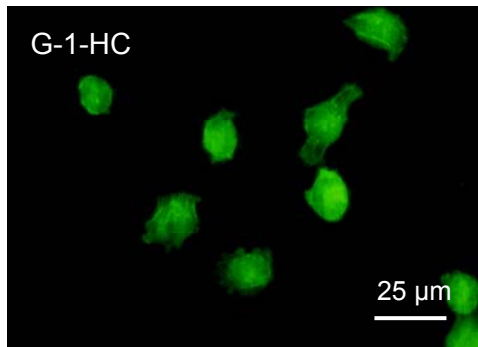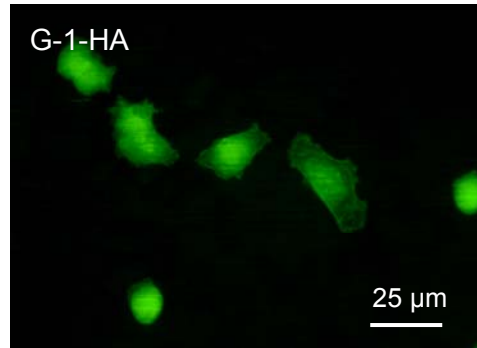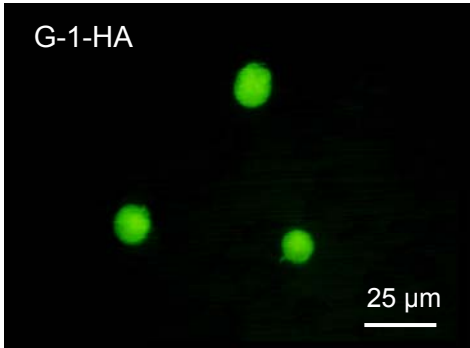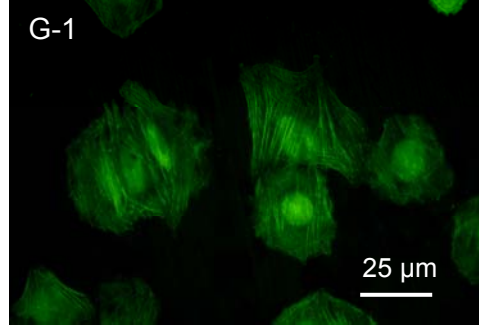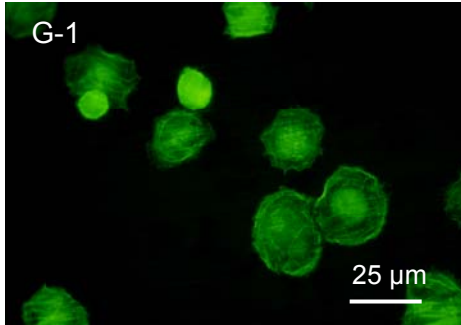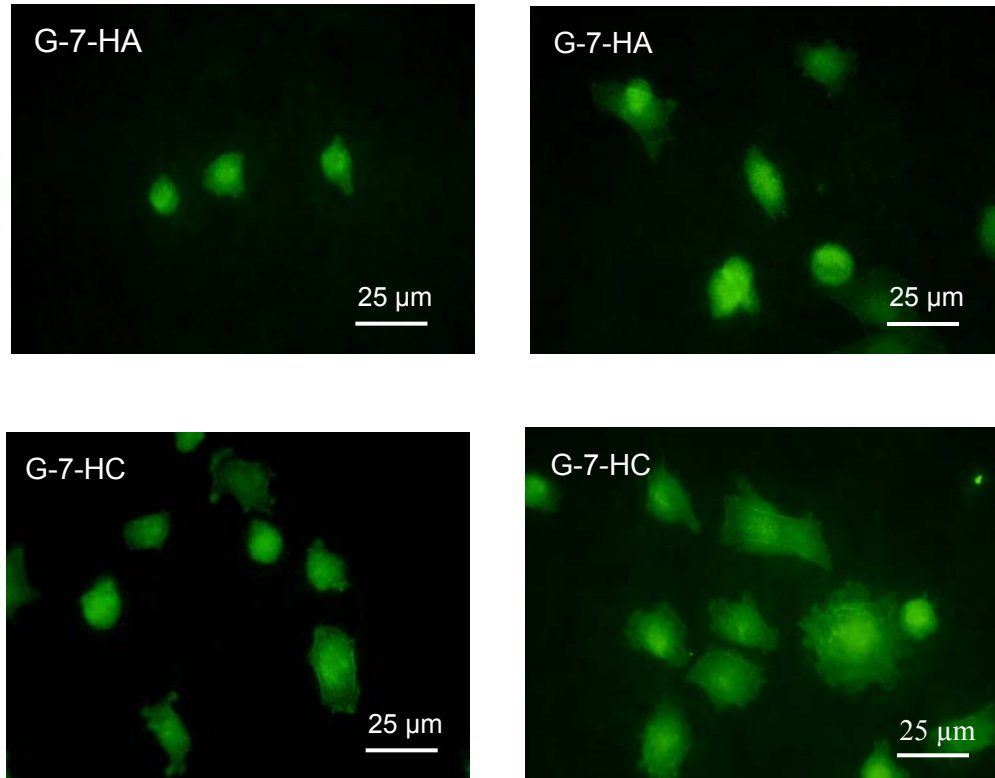
Figure 22 Actin cytoskeleton of cells cultured for 1(left) and 2 h (right) on the different surfaces of titanium was stained with phalloidin

To clarify the mechanism of cell reactions to nano HA and nano HA/collagen coatings, SEM was used to observe initial cell adhesion on both the coatings. Since the substrate below the coatings did not contact cells directly, cell responses actually did not demonstrate effects of characteristics of underlying substrates (Fig. 23). Since a nano HA coating covered the surface pores produced by anodic oxidation, the surface became more smooth and it leads to fewer sites for cell adhesion. However, cells still sensed any possible advantageous sites for their attachment. This is probably the main reason for lower cell adhesion on the nano HA-coated surfaces than on the underlying substrate such as G-7. Specially, cell adhesion to nano HA was strong enough to break the coating as cells were dried for SEM observation. The nano

HA/collagen-coated surface demonstrated remarkably more cell adhesion even though the coating covered the surface. Therefore, the results show collagen dissolved in the coating can enhance cell adhesion on the coating. On the other hand, cell on the nano HA/collagen-coated surface displayed more filopodia and extensions of the cytoplasmic membrane and this indicates the cells on the nano HA/collagen-coated surface have high motility. As a consequence, initial cell adhesion and behaviour, to a great extent, depend on surface structures and chemistry of the substrate to attach.
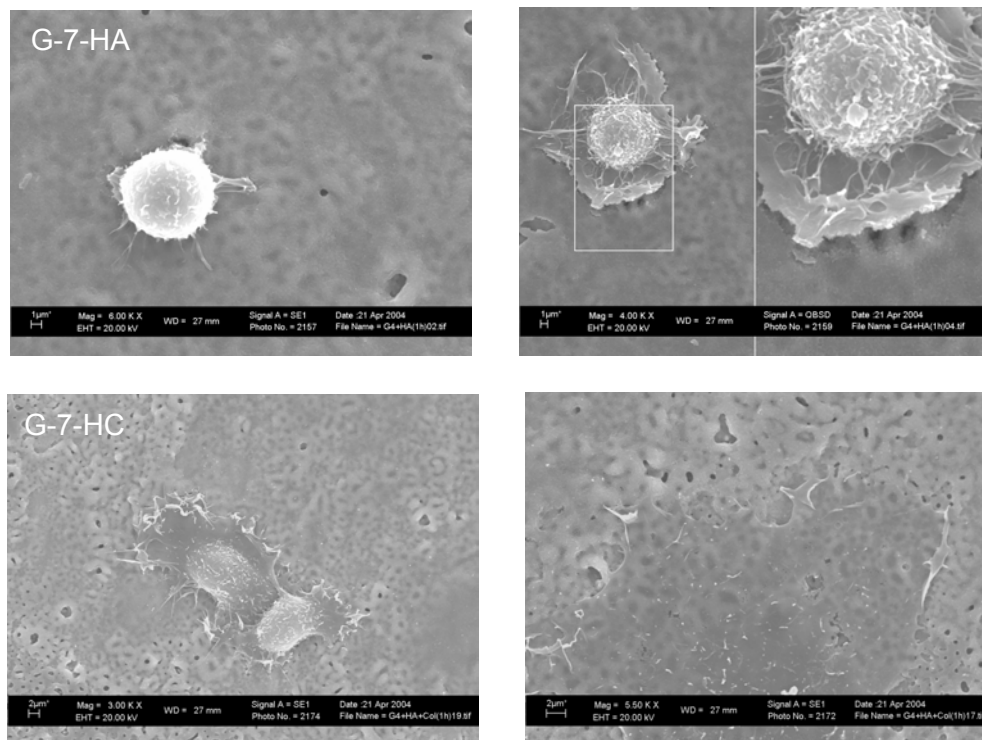
Figure 23 Morphology of cells on the nano HA and nano HA/collagen coatings for 1 hour

5 Discussion

5.1 Surface anodic oxides of titanium

5.1.1 Surface chemistry and topography of anodic oxides

The surface properties of an implant play a critical role in the biological responses it induces and its ultimate success. In the present study, anodic oxidation produces different topographies and chemical compositions of surface oxides on titanium. SEM analyses show micro-pores in the surface oxides of titanium except for the control and G-5. With an increase of anodizing voltages, the geometry of micro-pores in the anodic oxides increases in 0.2 M H_3PO_4 (up to ca. 0.5 μm) as well as in 0.03 M Ca-GP and 0.15 M CA (up to ca.2 μm). Phosphorus and calcium are incorporated into the surface oxide on titanium by anodic oxidation in different electrolytes. The XPS analyses show that the surface oxide of titanium is TiO_2, which, as reported before, is the predominant surface oxide on top of titanium and titanium alloys, and contains small amount of suboxides TiO and Ti_2O_3 closer to the metal/oxide interface [9]. The content of carbon in all the surfaces is about 20 at.% (30 at.% at most), which is much lower than that in the surfaces of most titanium implants (about 40 to 80 at.%) [94]. It is evident that the hydrocarbon cannot be present as a continuous overlayer even with carbon 43-45 at.%. Carbon contaminations on different oxides in our experimental groups were similar. Thus, though it cannot be ruled out that the results of our experiments are influenced by these contaminations to some extent, the described differences between the various anodized surfaces and the control are obviously due to the different oxides rather than to surface contaminations. In the present experiments, the comparatively low surface contamination is ascribed to the acid cleaning in the pre-treatment, anodizing and deionised-water washing, and particularly, acid cleaning and anodizing efficiently remove the outer layer formed during machining by etching or dissolving due to sparking in anodizing. From O 1s, P 2p and Ca 2p spectra, it is suggested that phosphorus in the anodised surfaces formed in both electrolytes be in the form of phosphate, and besides, calcium in the anodic oxides formed in electrolyte No.2 take the form of calcium phosphate. The existence states of calcium and phosphorus incorporated into the anodic oxides

are intimately associated with their sources, i.e. constitutes of electrolytes employed. Phosphorus is in the form of phosphate ions in electrolyte No.1. In electrolyte No.2, calcium glycerophosphate mainly consists of calcium α-glycerophosphate and calcium β-glycerophosphate, and both have calcium ions and phosphate groups in crystal structure [62]. Variation in chemical composition of the implant surface is acknowledged to affect cell attachment and proliferation. The absence of cytotoxicity documents the cytocompatibility of the surface oxides containing P or Ca and P in the present chemical states. The enhanced cell attachment and proliferation on these surfaces compared to those on the control surface further confirm their improved cytocompatibility. The observed positive effects *in vitro* may be due to the incorporation of phosphate ions or both calcium and phosphate ions, resulting in release of calcium and/or phosphate ions or molecules that can penetrate the cell membrane or activate membrane-bound receptors [69]. Besides, recent *in vivo* studies demonstrate a much higher percentage of bone contact for titanium implants with anodic oxides incorporated with both Ca and P or P, respectively, than the control [116, 119], and this is explained by the formation of biochemical bonding between bone and anodized surfaces incorporated with P and Ca in the bone-implant interface [119].

Cell attachment, spreading and subsequent proliferation are closely related to the surface properties of the substrate, e.g. composition, roughness, wettability and morphology. Besides chemical composition, as aforementioned, it is well known that surface roughness and morphology play an important role in biological responses of biomaterial surfaces. Surface roughness is enhanced by anodic oxides within the range of 0.1-0.5 μm and differs with anodizing voltages in two different electrolytes. The roughness variation can be explained by two contradictory mechanisms, i.e. decreasing roughness by removing grooves and increasing roughness by forming irregular pores. Thus, the increase of voltage leads to two possible results, i.e. decrease or increase of roughness, depending on which of the two contradictory mechanisms is dominant, that is, disappearance of grooves and pore formation. As anodising voltage increased, the decrease of roughness resulting from removing polishing grooves is beyond

the roughness increase derived from pores, whose contribution is weak due to small pore's diameter (ca. 0.5 µm at most) for electrolyte No. 1. In contrast, the pore formation led to an increase in roughness in electrolyte 2 due to much larger pores (diameter up to ca. 2 µm at 300 V) formed in this electrolyte.

Surface wettability may affect the attachment of cells either directly, since the attachment phase as an initial process involves physicochemical linkages between cells and surfaces including ionic forces, or indirectly through alterations in the adsorption of conditioning molecules, e.g. proteins. Increased wettability enhances interaction between implant surface and the biologic environment. Surface wettability is affected by not only by surface chemistry but also by topography parameters such as roughness and micro-texture. In the present work, all the surfaces are hydrophilic as the values of contact angles are in the range of 60 to 90°, which is similar to the other researchers' results [121]. This means that all the surfaces in the present study are conducive to cell attachment since it is revealed that mammalian cells can efficiently attach to hydrophilic surfaces in comparison with hydrophobic surfaces the cells inefficiently attach to. From the present experimental data, no correlation of contact angles and cell responses is demonstrated. A number of investigations have been undertaken on the influence of surface roughness on wettability parameters by static and dynamic contact angle measurements [81]. It is mainly concluded that roughness decreases the contact angle if the surface contact angle $\theta < 90°$ and increases the contact angle if $\theta > 90°$ [122]. The phenomenon that roughness decreases contact angles is also found in the present anodized surfaces except for G-5. This could be explained from the analysis of surface topography i.e. micro-texture and surface composition. Except for G-5, which indicates grooved morphology, all the other anodized surfaces are porous. For the porous surfaces, as Bico et al. [17] suggested, in the hydrophilic case, the water drop either follows the topography, which generates an efficient decreasing of the contact angle, or it spreads inside the pores, which also leads to the decrease of the contact angle.

Besides morphological parameters, surface composition should also be considered as a factor in the discussion of contact angles of the surface oxides.

Ions Ca^{2+} and PO_4^{3-}, as hydrophilic solutes in the surface oxides, promote surface hydration resulting in a decrease of contact angles. The compositional factor obviously has no effect in electrolyte No. 1, because the content of phosphate ions keeps almost constant in the oxides formed in this electrolyte. In electrolyte No 2, influence of the compositional effect can not be distinguished from morphological effectssince both Ca^{2+} and PO_4^{3-} contents in the oxides become higher by enhancing anodizing voltages, but this is also accompanied by an increase of roughness.

5.1.2 Enhancement of hydrophilicity by UV

In the present study, it is found that surface oxides on titanium show much higher hydrophilicity after UV irradiation than without UV exposure, either for native or anodic oxides.

It has been accepted that by UV irradiation, oxygen vacancies are most likely created at the two-coordinated bridging sites in TiO_2, resulting in the conversion of Ti^{4+} sites to Ti^{3+} sites, which favour dissociative water adsorption [130]. In the present work, anodic oxides were non-stoichiometric or even incorporated with Ca and P and different in topography (grooves and micro-pores) and structure including crystalline and amorphous oxides. Therefore, the findings in the present work have shown the phenomenon of photoinduced hydrophilicity on titanium oxide films over a wide range of composition, topography and structure, and however, its efficiency is affected by these parameters. The probable proposal for the mechanism for UV photoinduced hydrophilicity of anodic oxides on titanium is that UV irradiation creates oxygen vacancies in titanium oxides, thereby converting Ti cations from higher (e.g. IV, III) to lower valence(e.g. III, II), which facilitates water adsorption. As aforementioned, surface topography and composition have influence on the hydrophilicity, and it is most likely that they are involved in effects on UV induced hydrophilicity, too, thereby resulting in the distinct differences of hydrophilicity of the surface oxides. The effect of pores in surface oxides on titanium on photoinduced hydrophilicity is assumed to be that textured surfaces caused by pores, due to the larger actual area, which produces higher concentration of Ti cations of lower valence per unit

nominal area after UV irradiation. Consequently, pores enhance the effect of photoinduced hydrophilicity by UV irradiation on textured surfaces. On the other hand, as the content of calcium and phosphorus in surface oxides increases, Ti cations in the ratio of surface compositions become lower. Therefore, the efficiency of photoinduced hydrophilicity through Ti cations decreased with the enhancement of anodizing voltage or increase of Ca and P content. For native oxides in the flat surface, the oxide layer is thinner and has less actual surface area than porous surfaces, thereby producing fewer Ti cations of lower valence by UV exposure

5.1.3 Cell reactions to anodic oxides

Depending on the surface chemistry and physical characteristics of a biomaterial, cellular response to the material interface can be varied. Since anodic oxidation alters surface topography and incorporates some elements such as P or Ca/P into surface titanium oxides, cellular behaviours of these surfaces are distinctly different in the present study.

From statistical analysis, cell attachment distinctly shows different results with the change of surface roughness. In 0.2 M H_3PO_4, cell attachment on the anodized surfaces increases with a decrease in roughness. On the contrary, in 0.03 M Ca-GP and 0.15 M CA, cell attachment is increased as roughness is enhanced. However, attached cells on the surfaces anodized in either electrolyte increase with an increase in anodizing voltages, which are, in turn, associated with the thickness of the surface oxide. Similar contradictory phenomena have been also observed on titanium, i.e. the increase as well as decrease of osteoblast attachment and proliferation on rougher surfaces of titanium [96]. The disagreements between cell adhesion and surface roughness, in fact, further confirm that multiple characteristics of surface oxides of titanium are involved in cell responses. The thickness of the surface oxide, among the surface characteristics, is shown to be a main factor influencing the cell response besides surface roughness [29]. *In vivo* studies show that a high degree of bone contact and bone formation are achieved with titanium implants which are modified with respect to oxide thickness and surface topography [78],

and a significantly stronger bone response to anodic titanium oxides with 0.6-1.0 μm thickness than those with 0.2 μm or less thickness. Anodic oxide film thickness is linearly dependent on the applied voltage for titanium. As anodizing voltage increases, the thickness and crystallinity of the anodic oxides increase [146], and the thicker oxide with higher stability leads to favorable cell adhesion [71, 72]. In the present study, additionally, surface micro-pores of anodic oxides formed at higher anodizing voltages probably provide some benefits for cell attachment though the detailed mechanism has yet to be investigated. Consequently, cell attachment on the anodic oxides formed in 0.2 M H_3PO_4 is enhanced even with a little decrease in roughness. In 0.03 M Ca-GP and 0.15 M CA, in contrast, as anodizing voltage increases, the roughness, number of micro-pores and thickness as well as the crystallinity of anodic oxides gradually increase [145]. Hence, cell attachment is enhanced accompanying with the increase of roughness, micro-pores and thickness.

After the spherical cells attach on the surfaces, the following event for cell-substrate interaction is cell spreading. The substratum surface topography alters cell shape and modulates fibronectin at the transcriptional and post-transcriptional levels, as well as the amount of fibronectin assembly into the extracellular matrix [31]. It is reported that the surface texture of the Ti substrate can also affect the expression of fibronectin and vitronectin integrin receptors [59], modify their clustering or aggregation, and therefore determine variations in shape and spreading of cells [38]. During cell spreading, the shape of cells is changed and the cellular skeleton is reorganized. In our experiments, the shape of cells on the control surface and anodized surfaces is distinctly different, though the percentage of fully spread cells to total attached cells shows no statistical difference. This can be explained by the reason that cell spreading is affected by surface morphology or micro-topography. Most spread cells on the control surface after 1 hour are round, which is the same appearance as described on smooth surfaces [105], while the cells on the anodized titanium surface appeared more irregular and polygonal, covering a larger mean surface area, especially on G-4, G-7 and G-8. Since spreading is an essential step in cell adhesion prior to exponential growth phase [127], cell spreading can have a

profound effect on cell adhesion and growth. In fact we also see in our experiments that cell proliferation is enhanced by the oxide surfaces leading to a more rapid and distinct polygonal spreading of the cells. It is reported that cells appear to be under precise control by topographic guidance cues of various dimensions during morphogenesis [35]. However, little is known about the mechanisms whereby surface topography exerts its effects on cell shape and further growth.

In the present study, focal contacts on the control are more intensive than on anodized groups. Focal contacts act as a special structure of cell adhesion on the substrates, but in general, cells that form strong focal adhesions are less migratory. The shallow appearance of focal contacts on the more intensively anodized surfaces indicates that cell migration may be easier than on the control surface. Many more lamellipodia involved in cell migration are observed in cells on the more intensively anodized titanium than on the control. These phenomena indicate that the ability of cell migration on anodic oxides may be higher than that on the control and increases as anodizing voltage increases. In the present study, more stress fibers but fewer lamellipodia were formed on the control or weakly anodized surfaces. As a highly organized cytoskeleton with stress fibers is often associated with strong cell adhesion [10], the reorganization of the actin cytoskeleton, together with the results of the amount and distribution of focal contacts, further confirm the assumption that the cells on anodic oxides may have higher motility in comparison with those on the control.

The present results show, on the whole, that cell proliferation is enhanced by anodic oxidation. In 0.2 M H_3PO_4, rougher surfaces exhibit lower cell proliferation and this is consistent with the results from Martin et al. [90]. On the other hand, some researchers presented the different relationship, i.e. osteoblast proliferation could be enhanced on rougher surfaces [38]. In 0.03 M Ca-GP and 0.15 M CA, cell proliferation has no statistical difference except between G-5 and G-6. Therefore, cell proliferation is not only affected by roughness but also by surface micro-structure, composition and thickness of anodic oxides.

From the ALP activity in the present work, no apparent correlation is shown between surface characteristics and osteoblast differentiation. The contradictory relationship reported for cell proliferation or ALP activity and roughness can be ascribed to the sensitivity of osteoblasts to the surface features such as surface micro-topography [37].

Cells on G-1 are flat and more spread, and more focal contacts are observed around the periphery of the cells, whereas cells on the anodized surfaces are multipolar with ellipsoid nuclei but no discernible stress fibres. As culturing time increases, focal contacts of the cells on G-1 are elongated, e.g. from dots to dashes, and stress fibres increase in number and thickness. In fact, there is some correlation between the two types of focal contacts and stress fibres. Dots are the predominant type at the active edge of the cell, but are not associated with stress fibres, while dashes, which are elongated and large matured contacts, are associated with stress fibres [4]. Focal contacts are the loci of the shortest distance between cell and substrate, and they are also the sites of the stress fibre termination. They serve as coordination sites between cell adhesion and motility. The size of focal contacts is positively correlated with the attachment strength and inversely correlated with the migratory rate [7]. Enhanced focal adhesion is shown to have reduced cell motility [61]. Consequently, this indicates that cells on G-1 have a higher attachment strength and a lower motility than those on the porous anodic oxides. On the other hand, stress fibres anchor the cell and exert tension across the cell against the substrate on G-1, resulting in cell flattening, i.e. spreading. As solid actin bundles are involved in static, tension-generating cell-matrix interaction, stress fibres potentially counteract rather than favor cell migration. Therefore, the cells with well-organized stress fibres on G-1 are confirmed to be stationary (low motility). The cell nucleus is a dynamic structure and is structurally integrated with other elements of the cytoskeleton. Hence, the nucleus of the cell may passively extend when the cell spreads due to redistribution of mechanical forces across the nucleus matrix, the cytoskeletal filaments and the cell surface. The observed nuclear extensions also demonstrate the highly spread cells on G-1 compared to those on the anodized surfaces.

It has been shown that filopodia of varying lengths, transient structures extended from the cell body, play a vital role in cellular motility and guidance decisions for mammalian cells by sensing the molecular environment, developing adhesions, and transmitting signals that alter cellular motility [118]. The elongation and reorientation of filopodia are probably determined by guidance cues from the environmental signalling, e.g. the substrate structure. The present study demonstrates that initial cell reactions to different titanium surfaces, e. g. development of the actin-containing structures, namely focal contacts, point or dot contacts, and filopodia, are determined by different morphology of the surfaces in spite of their similar molecular composition.

Therefore, we suggest the following mechanisms of cell adhesion: For a smooth surface, repulsive signals from the environmental cues prevent extensions of the filopodia from the cell bodies. Thus, focal contacts are the main adhesion structures in the cell-substrate interaction. Furthermore, well-developed stress fibres exert tension across the whole cell bodies and flatten the cells on the substrate, seen as spreading of the cells and extension of cellular nuclei. Concerning the specimens structured in the micro- or submicrometre regime, first, filopodia transiently scan the substrate to sense the surface structures of titanium oxides. Secondly, a filopodium encounters either micro- or submicrometre structured pores acting as a favorable environment and stabilizing the cell according to the signals received during the pathfinding phase. Then, filopodia adapt to the surface structures to attach, enabling optimum anchorage by using specific points along the filopodia as well as their tips. Furthermore, the tips broaden and branch out to become localised adhesive structures (footpads). The subsequent cell spreading is mediated by cell membrane extensions at these footpads, or by protrusion of a cytoplasmic sheet, i.e. a lamella or a lamellipodium between adherent filopodia. Therefore, porous structures at either micro- or submicrometre scale supply positive guidance cues for anchorage-dependent cells to attach, leading to enhanced cell attachment. More evidence to support these proposed mechanisms is also found in recent experimental results [65, 149]: that cell reactions to the micro- and nanoporous oxide surfaces of titanium produced by acid etching,

sandblasting and anodizing, were similar to those to the micron- and submicron-scale porous surfaces in the present study. By these proposed mechanisms in the present study, it becomes evident that as the fractal dimensions of the substrate increase, the smaller becomes the contact area between the cell and substrate [4]. The osteoblasts are presumed to have higher motility on the anodized structures, compared to the control specimen G-1, since cell motility is generally associated with the protrusion of two types of actin-rich structures, namely lamellipodia and filopodia, at the leading edge of the cells.

5.2 Characterization and biological behaviours of nano HA and nano HA/collagen

5.2.1 Structure characteristics of nano HA

It is known that crystallinity of hydroxyapatite are probably affected by synthesis precursors, pH value, processes including aging temperature and time, and post-treatment. The lower dissolution rate of hydroxyapatite corresponds to higher crystallinity in aqueous solution or physiological fluids. If HA dissolves and degrades fast, it will result in the weakening of the coating-substrate bonding or the implant fixation to the host tissues [103]. In the present study, HA nanoparticles synthesized by a wet chemical method is relatively high in crystallinity and display a ellipsoid morphology, which is rather similar to needle-like shape of stoichiometric HA or non-stoichiometric apatite synthesized by other wet chemical methods. It is suggested the long axis of HA nanoparticles is parallel to [0001] [89] or perpendicular to the plane (002), which is also in agreement with the c-crystallographic (002) axis, i.e. strong preferred orientation of apatite crystals in bone. Aging temperature significantly enhances HA crystallinity, whereas aging time does not demonstrate any influence on their crystallinity. This phenomenon differs from the results reported by others using other calcium and phosphorus precursors, in which aging time effect became more pronounced as aging temperature increased, and this effect was ascribed to the increase of [H^+] concentration in the solution [82]. Therefore, the present nano HA, due to high crystallility and stability, should have relatively dissolution rate in human body fluid, and can be employed to improve the integrity and longevity of the coating layer.

From the results in the present study, it is assumed that the growth of HA particles is determined by the following chemical reaction rate, depending on the amount of energy of atoms or activation energy to ensure that the reaction proceeds.

$$10 \, Ca^{2+} + 6 \, PO_4^{3-} + 2 \, OH^- \rightarrow Ca_{10}(PO_4)_6(OH)_2$$
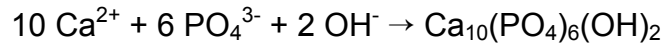
Quantitatively this relationship between the rate the above reaction proceeds and its temperature is determined by the Arrhenius Equation, i.e.

$$k = A \exp(-E/RT),$$

where k is the rate coefficient, A is a constant, E is the activation energy, R is the universal gas constant, and T is the temperature (in degrees Kelvin). Therefore, effects of aging temperature and time on crystallinity of HA nanoparticles are determined by a controlling factor in the formation of HA crystals, e.g. a reaction rate or atomic diffusion to arrange in order of crystals, the former is independent of time but temperature while the latter is a function of both temperature and time. The controlling factor is largely related to reactants or synthesis precursors.

It seems that annealing at different temperatures, i.e. from 300 to 900 °C, with a slow cooling rate, has no effect on structures of HA nanoparticles except for crystallinity from XRD results. In fact, since HA is a hydrated calcium phosphate, it begins to dehydroxylate at about 800°C to form oxy-hydroxyapatite. Furthermore, decomposition and reconstruction of nano HA occur during annealing and cooling in the temperature range of 1300- 1400 °C though these processes can not be demonstrated in XRD patterns.

5.2.2 Characterization and biological responses of nano HA and nano HA/collagen

The coating of titanium implants with a HA film is of particular interest because it allows for combining the mechanical strength of titanium substrate with the bioactive character of HA, improving both the biocompatibility of the implants

and the adhesion to bone. So far, commercially available HA coatings are deposited using a thick-plasma-spraying technique. These coatings are characterized by thickness from 50-200 µm, manifest poor shear stress, insufficient adherence to the substrate, inhomogeneous composition of a mixture of stoichiometric HA [$Ca_5OH(PO_4)_3$], whitlockite [$Ca_3(PO_4)_2$], amorphous calcium phosphate (ACP), and CaO, and risk of decohesion caused by partial dissolution of the ACP component of these relatively thick films. Among the possible alternatives, the sol-gel method is chosen for the homogeneous composition and uniform and fine microstructure of the resulting coating, as well as for the simplicity and low cost of this procedure. In the present study, nano HA and nano HA/collagen coatings on pure titanium or anodic titanium oxides significantly increase surface wettability or decrease contact angles, and in other words, nano HA coatings have higher surface energy and chemical reactivity, which are involved in biological responses to them. The nano HA and nano HA/collagen coatings belong to a smooth surface since their average roughness (Ra) is within 0.5 µm. However, these coatings demonstrate not very flat from distinctly diverse parameters such as Rmax and Rz and large standard deviations. Thus, the present coating procedure needs improving to obtain a flat surface.

Comparing to the underlying substrate, cells on the nano HA or nano HA/collagen coating show less initial cell attachment and spreading. This phenomenon is probably attributed to that initial cell adhesion largely depends on topography and surface chemistry, particularly topography. The formation of a multipolar shape for cells on the nano HA or nano HA coating results from stimulating plasma membrane along the border of cell body by nano HA. On one hand, cells demonstrate strong adhesion strength with nano HA and nano HA/collagen coatings. On the other hand, although cells with less spreading on the nano HA or nano HA/collagen coating, cells show higher mobility on those surfaces since cells connect to the surfaces by filopodia not focal contacts. In the present study, collagen remarkably benefits cell adhesion by enhancing initial cell attachment and spreading, and this is in agreement with others' [66]. Therefore the combination of collagen with nano HA provides a promising

coating for osteoblasts to adhere to. Besides, nano HA and collagen would play a role in promotion of osteoblast proliferation, differentiation and mineralization in the later stages of their interactions with osteoblasts.

In summary, nano HA/collagen, an analogue of bone, show a potential as coatings for titanium implants to improve osseointegration. In the present study, either nano HA or collagen indicates, to a certain extent, the ability to modulate cell behaviours during cell adhesion, and nano HA/collagen by combining both of them displays a sign of synergetic effect on cell responses. The present study only presents an initial step to investigate characteristics and biological responses of nano HA and nano HA/collagen. Much more work including further more *in vitro* and *in vivo* studies would be done to understand cell-nano HA/collagen interactions and apply nano HA/collagen for titanium implant surfaces in clinic medicine.

6 Conclusions

(1) Different porous surfaces of titanium were prepared by anodic oxidation in 0.2 M H_3PO_4, and in 0.03 M Ca-GP and 0.15 M CA, respectively. The anodic oxides contained P (ca.10 at.%) or Ca (1-6 at.%) and P (3-6 at.%) and their pores were at the micron and submicron-scale, respectively.

(2) Surface roughness was only a bit enhanced by anodic oxidation and contact angles of anodic oxides ranged from 60 to 90 °C. The wettability of anodic oxides displayed a trend opposite to roughness. XPS analysis show that calcium and phosphorus existed in anodic oxides as calcium phosphate and phosphate (PO_4^{3-}).

(3) It was found that UV irradiation significantly enhanced the wettability of titanium surface oxides, and the lower hydrophilicity the original surface has, the higher hydrophilic the surface would become after UV treatment.

(4) All the anodic oxides of titanium did not indicate cytotoxicity. Cell adhesion and proliferation were increased on anodic oxides, and the cells on anodic oxides showed irregular, polygonal growth and developed a number of lamellipodia and filopodia. In contrast, cells on the titanium surface showed more rounded and spread appearance with intense focal contacts and remarkable stress fibers. No correlation of ALP activity and the surface characteristics of the anodic oxides was demonstrated.

(5) Nano HA particles were synthesized in the range of 10-50 nm in size. The nano HA particles demonstrated relatively high crystallinity, which was increased as aging temperature increased but independent of aging time. Nano HA and nano HA/collagen coatings improved surface wettability and decreased surface roughness compared to the underlying surface, and showed a multipolar shape cells on them with some filopodia. Nano HA combined with collagen showed, to a certain extent, a sign of synergistic effect by significantly enhancing cell adhesion.

(6) Two mechanisms were proposed on cellular reactions to micron- and submicron-scale porous structures and a smooth surface of titanium. The porous structures could act as positive attachment sites for cellular filopodia in their interaction with cells. In comparison, cells on the smooth surface attach

and spread by focal contacts, acting as predominant adhesion structures in the cell-substrate interactions, around their periphery. These two mechanisms are applicable to other structures, e.g. grooves and pores, by different surface modifications and also may predict probable behaviours of cells *in vivo*.

7 References

1.   Aladjem A.(1973)
       Anodic oxidation of titanium and its alloys
       J Mater Sci 8, 688-704

2.   Albrektsson T.(1998)
       Hydroxyapatite-coated implants: a case against their use
       J Oral Maxillofac Surg 56, 1312-1326

3.   Albektsson T., Jacobsson M. (1987)
       Bone-metal interface in osseointegration
       J Prosthet Dent 57, 597-607

4.   Anselme K., Bigerelle M., Noel B., Dufresne E., Judas D., Iost A.,
       Hardouin P. (2000)
       **Qualitative and quantitative study of human osteoblast adhesion on
       materials with various surface roughnesses**
       J Biomed Mater Res 49,155-166

5.   Anselme K., Bigerelle M., Noel B., Iost A., Hardouin P. (2002)
       **Effect of grooved titanium substrate on human osteoblastic cell
       growth**
       J Biomed Mater Res 60, 529-540

6.   Aronsson B.O., Lausmaa J., Kasemo B. (1997)
       **Glow discharge plasma treatment for surface cleaning and
       modification of metallic biomaterials**
       J Biomed Mater Res 35, 49-73

7.   Arregui, C.O., Caronetto S., McKerracher L. (1994)
       **Characterization of neural cell adhesion sites: point contacts are
       the sites of interaction between integrins and the cytoskeleton in
       PC 12 cells**
       J Neurosci 14, 6967-6977

8.   Arys A., Philippart C., Dourov N., He Y., Le Q.T, Pireaux J.J. (1998)
       **Analysis of titanium dental implants after failure of osseointegration:
       combined histological, electron microscopy, and X-ray
       photoelectron
       spectroscopy approach**
       J Biomed Mater Res 43, 300-312

9.   Ask M., Lausmaa J., Kasemo B. (1988-89)
       **Preparation and surface spectroscopic characterization of oxide
       films on Ti6Al4V**
       Appl Surf Sci 35, 283-301

10. Badley R.A., Woods A., Carruthers L., Rees D.A. (1980)
Cytoskeletal changes in fibroblast adhesion and detachment
J Cell Sci <u>43</u>, 379-390

11. Baier R., Meyer A. (1988)
Implant surface preparation
Int J Oral Maxillofac Implants <u>3</u>, 9-12

12. Ball M.D., Downes S., Scotchford C.A., Antonov E.N., Bagratashvili V.N., Popov V.K., Lo W.J., Grant D.M., Howdle S.M. (2001)
Osteoblast growth on titanium foils coated with hydroxyapatite by pulsed laser ablation
Biomaterials <u>22</u>, 337-347

13. Ban S., Hasegawa J. (2002)
Morphological regulation and crystal growth of hydrothermal-electrochemically deposited apatite
Biomaterials <u>23</u>, 2965-2972

14. Baxter L.C., Frauchiger V., Textor M., ap Gwynn I., Richards R.G. (2002)
Fibroblast and osteoblast adhesion and morphology on calcium phosphate surfaces
European Cells and Materials <u>4</u>,1-17

15. Bergström K., Österberg E., Holmberg K., Hoffman A.S., Schuman T.P., Kozlovsky A., Harris J.H. (1994)
Effects of braching and molecular weight of surface-bound poly(ethylene oxide) on protein rejection
J Biomater Sci Polym Ed <u>6</u>,123-132

16. Berman A., Hanson H., Leiserowitz L., Koetzle T. F., Weiner S., Addadi L. (1993)
Biological control of crystal texture: a widespread strategy for adapting crystal properties to function
Science <u>259</u>, 776-779

17. Bico J., Thiele U., Quere D. (2002)
Wetting of textured surfaces
Colloids and Surfaces A: Physciochem Eng Aspects <u>206</u>, 41-46

18. Borgs C., De Coninck J., Kotecky R., Zinque M. (1995)
Does the roughness of the substrate enhance wetting?
Phys Rev Lett <u>74</u>, 2292-2294

19. Bowers K.T., Keller J.C., Randolph B.A., Wick D.G., Michaels C.M. (1992)
Optimization of surface micromorphology for enhanced osteoblast responses in vitro

Int J Oral Maxillofac Implants 7, 302-310

20.   Boyan B.D., Lincks J., Lohmann C.H., Sylvia V.L., Cochran K.L.
        Blanchard C.R., Dean D.D., Schwart Z. (1999)
        **Effect of surface roughness and composition on ostochondrocytes
        is dependent on cell maturation state**
        Journal of Orthopaedic Research 17, 446-457
        Int J Oral Maxillofac Implants 7, 302-310

21.   Brunette D.M. (2001)
        **Principles of cell behavior on titanium surfaces and their
        application to Implanted Devices**
        In: Brunette D.M., Tengvall P., Textor M., Thomsen P. (eds) Titanium in
        Medicine, Springer-Verlag, Berlin, p485-512

22.   Buser D., Schenk R.K., Steinemann S., Fiorellini J.P., Fox C.H., Stich H.
        (1991)
        **Influence of surface characteristics on bone integration of titanium
        implants. A histomorphometric study in miniature pigs**
        J Biomed Mater Res 25, 889-902

23.   Cambell C.E., Von Recum A.F. (1989)
        Microtopography and soft tissue response
        J Invest Surg 2, 51-74

24.   Carley A.F., Roberts J.C., Roberts M.W. (1990)
        **Dissociative chemisorption and localized oxidation states at
        titanium surfaces**
        Surf Sci 225, L39-L41

25.   Carlsson L.V., Alberktsson T., Berman C. (1989)
        Bone response to plasma-cleaned titanium implants
        Int J Oral Maxillofac Implants 4, 199-204

26.   Caulier H., van der Waerden J.P., Wolke J.G. (1997)
        **A histological and histomorphometrical evaluation of the
        application of screw-designed calcium phosphate (Ca-P)-coated
        implants in the cancellous maxillary bone of the goat**
        J Biomed Mater Res 35,19-30

27.   Chehroudi B., Gould T.R.L., Brunette D.M. (1989)
        **Effects of a grooved titanium-coated implant surface on epithelial
        cell behavior in vitro and in vivo**
        J Biomed Mater Res 23, 1067-1085

28.   Chehroudi B., Gould T.R., Brunette D.M. (1991)

A light and electron microscopic study of the effects of surface topography on the behavior of cells attached to titanium-coated percutaneous implants
J Biomed Mater Res 25, 387-405

29.   Chesmel K.D., Clark C.C., Brighton C.T., Black J. (1995)
Cellular responses to chemical and morphologic aspects os biomaterial surfaces.II. The biosynthetic and migratory response of bone cell populations.
 J Biomed Mater Res 29, 1101-1110.

30.   Cho S.A., Park K.T. (2003)
The removal torque of titanium screw inserted in rabbit tibia treated by dual acid etching
Biomaterials 24, 3611-3617

31.   Chou L., Firth J., Uitto V., Brunette D. (1995)
Substratum surface topography alters cell shape and regulates fibronectin mRNA level, mRNA stability,secretion and assembly in human fibroblasts
J Cell Sci 108, 1563-1573

32.   Chusuei C.C., Goodman D.W.C., Goodman D. W., Van Stipdonk M. J., Justes D. R., Schweikert, E. A. (1999)
Calcium phosphate phase identification using XPS and time-of-flight cluster SIMS
Anal Chem 71,149-153

33.   Clark P., Connolly P., Curtis A.S. (1990)
Topographical control of cell behaviour:II. Multiple grooved substrata
Development 108, 635-644

34.   Cochran D., Simpson J., Weber H., Buser D. (1994)
Attachment and growth of periodontal cells on smooth and rough titanium
Int J Oral Maxillofac Implants 9, 289-297

35.   Curtis A.S.G, Clark P. (1990)
The effect of topographic and mechanical properties of materials on cell behaviour
Crit Rev Biocomp 5, 343-362

36.   Curtis A., Wilkinson C. (1997)
Topographical control of cells
Biomaterials 18, 1573-1583

37.   Davies J.E., Lowenberg B., Shiga A. (1990)

The bone-titanium interface in vitro
J Biomed Mater Res <u>24</u>, 1289-1306

38.   Degasne I., Basle M.E, Demais V., Hure G., Lesourd M., Grolleau B.,
       Mercier L., Chappard D. (1999)
       **Effects of roughness, fibronectin and vitronectin on attachment,
       spreading, and proliferation of human osteoblast-like cells (Saos-2)
       on titanium surface**
       Calcif Tissue Int <u>64</u>, 499-507

39.   den Braber E.T., Jansen H.V., de Boer M.J., Croes H.J, Elwenspoek M,
       Ginsel   L.A., Jansen J.A. (1998)
       **Scanning electron microscopic, transmission electron microscopic,
       and confocal laser scanning microscopic observation of fibroblasts
       cultured on microgrooved surfaces of bulk titanium substrata**
       J Biomed Mater Res <u>40</u>, 425-433

40.   den Braber E.T., de Ruijter J.E., Ginsel L.A., von Recum A.F., Jansen
       J.A.   (1998)
       **Orientation of ECM protein deposition, fibroblast cytoskeleton, and
       attachment   complex   components   on   silicone   microgrooved
       surfaces**
       J Biomed Mater Res <u>40</u>, 291-300

41.   Dennison D.K, Huerzeler M.B, Quinones C, Caffesse R.G. (1994)
       **Contaminated implant surfaces: an in vitro comparison of implant
       surface coating and treatment modalities for decontamination**
       J Periodontol <u>65</u>, 942-948

42.   Dieudonne S.C., van den Dolder J., de Ruijter J.E., Paldan H., Peltola T.,
       van Hof M.A., Happonen R.P., Jansen J.A.(2002)
       **Osteoblast differentiation of bone marrow stromal cells cultured on
       silica gel and sol-gel-derived titania**
       Biomaterials <u>23</u>, 3041-3051

43.   Dupraz A., Nguyen T.P., Richard M., Daculsi G., Passuti N. (1999)
       **Influence of a cellulosic ether carrier on the structure of biphasic
       calcium phosphate ceramic particles in an injectable composite
       material**
       Biomaterials <u>20</u>, 663-673

45.   Eliades T. (1997)
       **Passive films growth on titanium alloys: physicochemical and
       biological
       Considerations**
       Int J Oral Maxillofac Implants <u>12</u>, 621-627

46.   Fernandez-Pradas J.M., Cleries L., Martinez E., Sardin G., Esteve J.,

Morenza J.L. (2001)
Influence of thickness on the properties of hydroxyapatite coatings deposited by KrF laser ablation
Biomaterials <u>22</u>, 2171-2175

47. Garcia-Alonso M.C., Saldana L, Valles G, Gonzalez-Carrasco J.L, Gonzalez- Cabrero J, Martinez M.E, Gil-Garay E, Munuera L(2003)
In vitro corrosion behaviour and osteoblast response of thermally oxidised Ti6Al4V alloy
Biomaterials <u>24</u>, 19-26

48. Geissler U., Hempel U., Wolf C., Scharnweber D., Worch H., Wenzel K.W. (2000)
Collagen type I-coating of Ti6Al4V promotes adhesion of osteoblasts
J Biomed Mater Res <u>51</u>, 752-760

49. Giavaresi G., Ambrosio L., Battiston G.A., Casellato U., Gerbasi R., Finia M., Aldini N.N., Martini L., Rimondini L., Giardino R.(2004)
Histomorphometric, ultrastructural and microhardness evaluation of the osseointegration of a nanostructured titanium oxide coating by metal-organic chemical vapour deposition: an in vivo study
Biomaterials <u>25</u>, 5583-5591

50. Goldberg V., Stevenson S., Feighan J., Davy D. (1995)
Biology of grit-blasted titanium alloy implants
Clin Orthop <u>319</u>, 122-129

51. Grinell F. (1978)
Cellular adhesiveness and extracellular substrata
Int Rev Cytol <u>53</u>, 65-144.

52. Gruner H. (2001)
Thermal spray coatings on titanium
In: Brunette D.M., Tengvall P.,Textor M., Thomsen P. (eds) Titanium in Medicine, Springer-Verlag, Berlin, pp375-416

53. Hallab N.J., Bundy K.J., O'connor K., Moses R.L., Jacobs J.J. (2001)
Evaluation of metallic and polymeric biomaterial surface energy and surface roughness characteristics for directed cell adhesion
Tissue Engineering <u>7</u>, 55-71

54. Hamad K., Kon M., Hanawa T., Yokoyama K., Miyamoto Y., Asaoka K. (2002)
Hydrothermal modification of titanium surface in calcium solutions
Biomaterials <u>23</u>, 2265-2272

55. Hanawa T., Ota M. (1992)

Characterization of surface film formed on titanium in electrolyte using XPS
Appl Surf Sci <u>55</u>, 269-276

56.   Hench L.L. (1998)
Bioceramics
J Am Ceram Soc <u>81</u>,1705-1728

57.   Hench L.L., Ethridge E.C. (1982)
Biomaterials: An Interfacial Approach
Biophysics and Bioengineering Series, ed. A, Noordergraaf, Academic Press, New York, vol.4, p.139.

58.   Homsy C.A.(1973)
Implant stabilization. Chemical and biochemical consideration
Orthop Clin North Am <u>4</u>, 295-311

59.   Hormia M, Kononen M. (1994)
Immunolocalization of fibronectin and vitronection receptors in human gingival fibroblasts spreading on titanium surfaces
J Periodontal Res <u>29</u>, 146-152

60.   Hure G., Donath K., Lesourd M., Chappard D., Basle M.F. (1996)
Does titanium surface treatment influence the bone-implant interface? SEM and histomorphometry in a 6-month sheep study
Int J Oral Maxillofac Implants <u>11</u>, 506-511

61.   Ilic D., Furuta Y., Kanazawa S., Takeda N., Sobue K., Nakatsuji N., Nomura S., Fujimoto J., Okada M., Yamamoto T. (1995)
Reduced cell motility and enhanced focal adhesion contact formation in cells from FAK-deficient mice
Nature 377, 539-544

62.   Inoue M, In Y, Ishida T. (1992)
Calcium bionding to phospholid: Structural study of calcium glycerophosphyte
J Lipid Res <u>33</u>, 985-994

63.   Jallot E., Benhayoune H., Kilian L., Irigaray J.L., Oudadesse H., Balossier G., Bonhomme P. (2000)
STEM and EDXS characterization of physicochemical reactions at the interface between a bioglass coating and bone
Surface and Interface Analysis <u>29</u>, 314-320

64.   Jayaraman M., Meyer U., Buehner M., Joos U., Wiesmann H.P.(2004)
Influence of titanium surfaces on attachment of osteoblast-like cells in vitro
Biomaterials <u>25</u>, 625-631

65. Jinno T., Kirk S.K., Morita S., Goldberg V.M. (2004)
Effects of calcium ion implantation on osseointegration of surface-blasted titanium alloy femoral implants in a canine total hip arthroplasty model
J Arthroplasty 19, 102-109

66. Jokinen J., Dadu E., Nykvist P., Kapyla J., White D.J., Ivaska J., Vehvilainen P., Reunanen H., Larjava H., Hakkinen L., Heino J. (2004)
Integrin-mediated cell adhesion to type I collagen fibrils
J Biol Chem 279, 31956-31963

67. Jonasova L., Muller F.A, Helebrant A., Strnad J., Greil P. (2004)
Biomimetic apatite formation on chemically treated titanium
Biomaterials 25, 1187-1194

68. Kasemo B. (2002)
Biological surface science
Surf Sci 500, 656-677

69. Kasemo B., Gold J. (1999)
Implant surfaces and interface processes
Adv Dent Res 13, 8-20

70. Keller J.C, Draughn R.A, Wightman J.P, Dougherty W.J, Meletiou S.D. (1990)
Characterization of sterilized CP titanium implant surfaces
Int J Oral Maxillofac Implants 5, 360-367

71. Keller J.C, Stanford C.M., Wightman J.P., Draughn R.A, Zaharias R. (1994)
Characterization of titanium implant surfaces. III
J Biomed Mater Res 28, 939-946

72. Kieswetter K., Schwartz Z., Dean D.D, Boyan B.D. (1996)
The role of implant surface characteristics in the healing of bone
Crit Rev Oral Biol Med 7, 329-345

73. Kieswetter K., Schwartz Z., Hummert T.W., Cochran D.L., Simpson J., Dean D.D., Boyan B.D. (1996)
Surface roughness modulates the local production of growth factors and cytokines by osteoblast-like MG-63 cells
J Biomed Mater Res 32, 55-63

74. Kim H.M., Miyaji F, Kokubo T, Nishiguchi S, Nakamura T(1999)
Graded surface structure of bioactive titanium prepared by chemical treatment
J Biomed Mater Res 45, 100-107

75.   Klawitter J.J., Hulbert S.F. (1971)
Application of porous ceramics for the attachment of load-bearing orthopaedic applications
J Biomed Mater Res 2, 161-229

76.   Klein C.P.A.T., Wolke J.G.C., Blieck-Hogervorst J.M.A., de Groot Kd. (1994)
Calcium phosphate plasma-sprayed coatings and their stability: an in-vivo study
J Biomed Mater Res 28: 909–917

77.   Krupa D., Baszkiewicz J., Kozubowski J.A., Barcz A., Sobczak J.W., Bilinski A., Lewandowska-Szumiel M., Rajchel B. (2002)
Effect of phosphorus-ion implantation on the corrosion resistance and biocompatibility of titanium
Biomaterials 23, 3329-40

78.   Larsson C., Thomsen P., Aronsson B.O., Rodahl M., Lausmaa J., Kasemo B., Ericson L.E. (1996)
Bone response to surface-modified titanium implants: studies on the early tissue response to machined and electropolished implants with different oxide thicknesses
Biomaterials 17, 605-616

79.   Lassen B., Holmberg K., Brink C., Carlen A., Olsson J. (1994)
Binding of salivary proteins and oral bacteria to hydrophobic and phdrophilic surfaces in vivo and in vitro
Colloid Polym Sci 272,1143-1150

80.   Li J., Liao H., Fartash B., Hermannsson L., Johnsson T. (1997)
Surafce-dimpled commercially pure titanium implant and bone ingrowth
Biomaterials 18, 691-696

81.   Lim Y.J., Oshida Y., Andres C.J., Barco M.T(2001)
Surface characterizations of variously treated titanium materials
Int J Oral Maxillofac Implants 16, 333-342

82.   Liu D.M., Troczynski T., Tseng W.J. (2002)
Aging effect on the phase evolution of water-based sol-gel hydroxyapatite
Biomaterials 23, 1227-1236

83.   Lo W.J, Grant D.M., Ball M.D., Welsh B.S., Howdle S.M., Antonov E.N., Bagratashvili V.N., Popov V.K. (2000)

Physical, chemical, and biological characterization of pulsed laser deposited and plasma sputtered hydroxyapatite thin films on titanium alloy
J Biomed Mater Res 50, 536-545

84.   Lu G., Bernasek S.L., Schwartz J. (2000)
Oxidation of a polycrystalline titanium surface by oxygen and water
Surf Sci 458, 80-90

85.   Lugscheider E., Knepper M., Heimberg B. (1994)
Cytotoxicity investigation of plasma-sprayed calcium phosphate coatings
J Mater Sci Mater Med 5, 371–5

86.   Lusquinos F., De Carlos A., Pou J., Arias J.L., Boutinguiza M., Leon B., Perez-Amor M., Driessens F.C., Hing K., Gibson I., Best S., Bonfield W. (2003)
Calcium phosphate coatings obtained by Nd: YAG laser cladding: physicochemical and biologic properties
J Biomed Mater Res 64A, 630-637

87.   Maitz M.F., Pham M.T., Wieser E., Tsyganov I. (2003)
Blood compatibility of titanium oxides with various crystal structure and element doping
J Biomater Appl 17, 303-319

88.   Malmsten M., Lassen B., van Alstine J.M., Nilsson U.R. (1996)
Adsorption of complement protein C3 and C1q
J Colloid Interface Sci 178,123-134

89.   Mao C., Li H., Cui F., Ma C., Feng Q. (1999)
Oriented growth of phosphates on poly crystalline titanium in a process mimicking biomineralization
J Cryst Growth 206, 308-312

90.   Martin J.Y., Schwartz Z., Hummert T.W., Schraub D.M., Simpson J., Lankford J.Jr., Dean D.D., Cochran D.L., Boyan B.D. (1995)
Effect of titanium surface roughness on proliferation, differentiation, and protein synthesis of human osteoblast-like cells (MG63)
J Biomed Mater Res 29, 389-401

91.   McCracken M. (1999)
Dental implant materials: commercially pure titanium and titanium alloys
Journal of Prosthodontics 8, 40-43

92.   Milella E., Cosentino F., Licciulli A., Massaro C.(2001)

Preparation and characterisation of titania/hydroxyapatite composite coatings obtained by sol-gel process
Biomaterials <u>22</u>, 1425-1431

93. Miyakawa O., Watanabe K., Okawa S., Kanatani M., Nakano S., Kobayashi M. (1996)
Surface contamination of titanium by abrading treatment
Dent Mater J <u>15</u>, 11-21

94. Morra M., Cassinelli C., Bruzzone G., Carpi A., Santi G.D., Giardino R., Fini M. (2003)
Surface chemistry effects of topographic modification of titanium dental implant surfaces : 1. Surface analysis
Int J Oral Maxillofacial Implants <u>18</u>, 40-45

95. Morris H.F., Ochi S. (1998)
Hydroxyapatite-coated implants: a case for their use
J Oral Maxillofac Surg <u>56</u>,1303-1311

96. Mustafa K., Wennerberg A., Wroblewski J., Hultenby K., Lopez B.S., Arvidson K. (2001)
Determining optimal surface roughness of TiO$_2$ blasted titanium implant material for attachment, proliferation and differentiation of cells derived from human mandibular alveolar bone
Clin Oral Impl Res <u>12</u>, 515-525

97. Nakahara H, Goldberg V.M., Caplan A.I.(1992)
Culture-expanded periosteal derived cells exhibit osteo-chondrogenic potential in porous calcium phosphate ceramics in vivo
Clin Orthop Rel Res <u>276</u>, 291-298

98. Nayab S.N., Jones F.H., Olsen I. (2004)
Human alveolar bone cell adhesion and growth on ion-implanted titanium
J Biomed Mater Res <u>69A</u>, 651-657

99. Nguyen H.Q., Deporter D.A., Pilliar R.M., Valiquette N, Yakubovich R.(2004)
The effect of sol-gel-formed calcium phosphate coatings on bone ingrowth and osteoconductivity of porous-surfaced Ti alloy implants
Biomaterials <u>25</u>, 865-876

100. Okamoto K, Matsuura T, Hosokawa R, Akagawa Y. (1998)
RGD peptides regulate the specific adhesion scheme of osteoblasts to hydroxyapatite but not to titanium
J Dent Res <u>77</u>, 481-487

101. Okumura A., Goto M., Goto T., Yoshinari M., Masuko S., Katusuki T., Tanaka T.(2001)
      Substrate affects the initial attachment and subsequent behaviour of human osteoblastic cells (Saos-2)
      Biomaterials 22, 2263-2271

102. Olson S, Arzate H, Narayanan AS, Page RC. (1991)
      Cell attachment activity of cementum proteins and mechanism of endotoxin inhibition
      J Dent Res 70, 1272-1277

103. Overgaard S., Soballe K., Hansen E.S., Joesphsen K., Bunger C. (1996)
      Implant loading accelerates adsorption of hydroxyapatite coating
      J Orthop Res 14, 888-894

104. Pan J., Liao H., Leygraf C., Thierry D., Li J. (1998)
      Variation of oxide films on titanium induced by osteoblast-like cell culture and the influence of an H_2O_2 pretreatment
      J Biomed Mater Res 40, 244-256

105. Parham P.L Jr, Cobb C.M, French A.A, Love J.W, Drisko C.L, Killoy W.J. (1989)
      Effects of an air-powder abrasive system on plasma-sprayed titanium implant surfaces: an in vitro evaluation
      J Oral Implantol 15, 78-86

106. Pearson B.S, Klebe R.J, Boyan B.D, Moskowicz D. (1988)
      Comments on the clinical application of fibronectin in dentistry
      J Dent Res 67, 515-517

107. Perizzollo D, Lacefield W.R., Brunette., D.M. (2001)
      Interaction between topography and coating in the formation of bone nodules in culture for hydroxyapatite- and titanium-coated micromachine surfaces
      J Biomed Mater Res 56, 494–503

108. Pham M.T., Matz W., Reuther H., Richter E., Steiner G., Oswald S.(2002)
      Interface-mediated synthesis of hydroxyapatite
      J Biomed Mater Res 59, 254-258

109. Pilliar R.M. (1987)
      Porous surfaced metallic-implants for orthopaedic applications
      J Biomed Mater Res Appl Biomater 21,1-33

110. Pilliar R.M. (1998)

Overview of surface variablity of metallic endosseous dental implants: textured and porous surface-structured designs
Implant Dent 7, 305-314

111. Price N., Bendall S.P., Frondoza C., Jinnah R.H., Hungerford D.S. (1997)
Human osteoblast-like cells (MG63) proliferate on a bioactive glass surface
J Biomed Mater Res 37, 394-400

112. Sawase T., Wennerberg A., Baba K., Tsuboi Y., Sennerby L., Johansson C.B., Albrektsson T. (2001)
Application of oxygen ion implantation to titanium surfaces: effects on surface characteristics, corrosion resistance, and bone response
Clin Implant Dent Relat Res 3, 221-229

113. Shams el Din A.M., Hammond A. A. (1988)
Oxide film formation and thickening of titanium in water
Thin Solid Films 167, 269-280

114. Sham T.K., Lazarus M.S. (1979)
X-ray photoelectron spectroscopy (XPS) studies of clean and hydrated TiO_2 (rutile) surfaces
Chem Phys Lett 68, 426-432

115. Smith D.C, Lugowski S, McHugh A, Deporter D, Watson P.A, Chipman M. (1997)
Systemic metal ion levels in dental implant patients
Int J Oral Maxillofac Implants 12, 828-834

116. Son W.W., Zhu X., Shin H.I, Ong J.L., Kim K.H. (2003)
In vivo histological response to anodized and anodized/ hydrothermally treated titanium implants
J Biomed Mater Res 66B, 520-525

117. Stangl R., Rinne B., Kastl S., Hendrich C. (2001)
The influence of pore geometry in cp Ti-implants a cell culture investigation
European Cells and Materials 2, 1-9

118. Steketee M., K.Balazovich, K.W.Tosney (2001)
Filopodial initiation and a novel filament-oganizing center, the focal ring
Mol Biol Cell 12, 2378-2395

119. Sul Y.T.(2003)
The significance of the surface properties of oxidized titanium to the bone response: special emphasis on potential biochemical

bonding of oxidized titanium implant
Biomaterials <u>24</u>, 3893-3907

120.   Sun L., Berndt C.C., Gross K.A., Kucuk A. (2001)
Material fundamentals and clinical performance of plasma-sprayed hydroxyapatite coatings: a review
J Biomed Mater Res <u>58</u>, 570-592

121.   Takebe J., Itoh S., Okada J., Ishibashi K. (2000)
Anodic oxidation and hydrothermal treatment of titanium results in a surface that causes increased attachment and altered cytoskeletal morphology of rat bone marrow stromal cells in vitro
J Biomed Mater Res <u>51</u>, 398-407

122.   Takeuchi M., Abe Y., Yoshida Y., Nakayama Y., Okazaki M., Akagawa Y. (2003)
Acid pretreatment of titanium implants
Biomaterials <u>24</u>, 1821-1827

123.   Thomas K.A., Cook S.D. (1985)
An evaluation of variables influencing implant fixation by direct bone apposition
J Biomed Mater Res <u>19</u>, 875-901

124.   Thull R., Grant D. (2001)
Physical and chemical vapor deposition and plasma-assisted techniques for coating titanium
In:Brunette D.M., Tengvall P., Textor M., Thomsen P. (eds) Titanium in Medicine, Springer-Verlag, Berlin, pp283-341

125.   Vercaigne S,Wolke J.G.C., Naert I., Jansen J.A. (2000)
A histological evaluation of TiO$_2$ gritblasted and Ca-P magnetron sputtered coated implants placed in the trabecular bone of the goat: part 2
Clinical Oral Implants Research <u>11</u>,314–324

126.   Vezeau P.J, Koorbusch G.F, Draughn R.A, Keller J.C. (1996)
Effects of multiple sterilization on surface characteristics and in vitro biologic responses to titanium
J Oral Maxillofac Surg <u>54</u>, 738-746

127.   Vogler E.A., Bussian R.W. (1987)
Short-term cell-attachment rates. A surface-sensitive test of cell-substrate compatibility
J Biomed Mater Res <u>21</u>, 1197-1211

128.   Walboomers X.F., Croes H.J.E., Ginsel L.A., Jansen J.A. (1999)
Contact guidance of rat fibroblasts on varous implant materials

J Biomed Mater Res <u>47</u>, 204-212

129. Walboomers X.F., Ginsel L.A., Jansen J.A.(2000)
Early spreading events of fibroblasts on microgrooved substrates
J Biomed Mater Res <u>51</u>, 529-534

130. Wang R., Hashimoto K., Fujishima A., Chikuni M., Kojima E., Kitamura A., Shimohigoshi M., Watanabe T. (1998)
Photogeneration of Highly Amphiphilic TiO$_2$ Surfaces
Advanced Materials <u>10</u>,135-138

131. Weiss R.E, Reddi A.H. (1981)
Appearance of fibronectin during the differentiation of cartilage, bone and bone marrow
J Cell Biol <u>88</u>, 630-636

132. Welin-Klingström S., Askendal A., Elwing H. (1993)
Surfactant and protein interactions on wettability gradient surfaces
J Colloid Interface Sci <u>158</u>, 188-194

133. Wen H.B., de Wijn J.R., Cui F.Z., de Groot K. (1998)
Preparation of calcium phosphate coatings on titanium implant materials by simple chemistry
J Biomed Mater Res <u>41</u>, 227-236

134. Wennerberg A., Albrektsson T., Andersson B., Krol J.J. (1995)
A histomorphometric and removal torque study of screw-shaped titanium implants with three different surface topographies
Clin Oral Implants Res <u>6</u>, 24-30

135. Wennerberg A., Albrektsson T., Johansson C., Andersson B. (1996)
Experimental study of turned and grit-blasted screw-shaped implants with special emphasis on effects of blasting material and surface topography
Biomaterials <u>17</u>, 15-22

136. Wennerberg A, Bolind P, Albrektsson T. (1991)
Glow charge pretreated implants combined with temporary bone tissue ischemia
Swed Dent J <u>15</u>, 95-101

137. Wilkinson C.D.W., Curtis AS.G., Crossan J. (1998)
Nanofabrication in cellular engineering
J Vac Sci Technol <u>B16</u>, 3132-3136

138. Wojciak-Stothard B., Madeja Z., Korohoda W., Curtis A., Wilkinson C. (1995)

Activation of macrophage-like cells by multiple grooved substrata. Topographical control of cell behaviour
Cell Biol Int <u>19</u>, 485-490

139. Wolke J.G., van Dijk K., Schaeken H.G., de Groot K., Jansen J.A. (1994)
Study of the surface characteristics of magnetron-sputter calcium phosphate coatings
J Biomed Mater Res <u>28</u>, 1477-1484

140. Xiao S.J., Kenausis G., Textor M. (2001)
Biochemical modification of titanium surfaces
Titanium in Medicine (Brunette DM, Tengvall P, Textor M, Thomsen P. eds), Springer-Verlag, Berlin, 417-455

141. Xynos L.D., Edgar A.J., Buttery L.D.K., et al.(2001)
Gene expression profiling of human osteoblasts following treatment with the ionic products of Bioglass 45S5
J Biomed Mater Res <u>55</u>, 151-157

142. Yliheikkila P.K., Masuda T., Ambrose W.W., Suggs C.A., Felton D.A., Cooper L.F. (1996)
Preliminary comparison of mineralizing multilayer cultures formed by primary fetal bovine mandibular osteoblasts grown on titanium, hydroxyapatite, and glass substrates
Int J Oral Maxillofac Implants <u>11</u>, 456-465

143. Zablotsky M.H, Wittrig E.E, Diedrich D.L, Layman D.L, Meffert R.M. (1992)
Fibroblastic growth and attachment on hydroxyapatite-coated titanium surfaces following the use of various detoxification modalities. Part II: Contaminated hydroxyapatite
Implant Dent <u>1</u>,195-202

144. Zeng H., Lacefield W.R., Mirov S. (2000)
Structural and morphological study of pulsed laser deposited calcium phosphate bioceramic coatings: influence of deposition conditions, laser parameters, and target properties
J Biomed Mater Res <u>50</u>, 248-258

145. Zhu X., Kim K., Jeong Y. (2001)
Anodic oxide films containing Ca and P of titanium biomaterial
Biomaterials <u>16</u>, 2199-2206

146. Zhu X., Kim K., Ong J.L., Jeong Y. (2002)
Surface analysis of anodic oxide films containing phosphorus on titanium
Int J Oral Maxillofac Implants <u>17</u>, 331-336

147. Zhu X., Ong J.L., Kim S.Y., Kim K. H.(2002)

Surface characteristics and structure of anodic oxide films containing Ca and P on a titanium implant material
J Biomed Mater Res <u>60</u>, 333-338

148. Zhu X., Ong J.L., Kim S.Y., Kim K.H.(2003)
Characterization of hydrothermally treated anodic oxides containing Ca and P on titanium
J Mater Sci Mater Med <u>14</u>, 621-634

149. Zinger O., Anselme K., Denzer A., Habersetzer P., Wieland M., Jeanfils J., Hardouin P.,Landolt D. (2004)
Time-dependent morphology and adhesion of osteoblastic cells on titanium model surfaces featuring scale-resolved topography
Biomaterials <u>25</u>, 2695-2910

8 Publications

1. Zhu X., Chen J., Scheideler L., Reichl R., Geis-Gerstorfer J. (2004)
    Effects of topography and composition of titanium surface oxides on osteoblast responses
    Biomaterials <u>25</u>, 4087-4103

2. Zhu X., Chen J., Scheideler L., Schille C., Geis-Gerstorfer J. (2003)
    In Vitro Osteoblast Responses to Anodic Oxides Containing Ca and P on Titanium
    J Dent Res <u>82</u>(B-308), 2379

3. Zhu X., Chen J., Scheideler L., Altebaeumer T., Geis-Gerstorfer J., Kern D.T. (2004)
    Cellular reactions of osteoblasts to micron and submicroscale structures of titanium surfaces
    Cells Tissues Organs <u>178</u>, 13-22

4. Zhu X., Rupp F., Geis-Gerstorfer J.
    A novel approach to control hydrophilicity of surface oxides on titanium
    Submitted

5. Zhu X., et al.
    Structure characterization and cell adhesion of nano HA
    In preparation

6. Zhu X., et al.
    Surface characterization and cell behaviours of nano HA/collagen
    In preparation

9 Acknowledgements

I would like to express the sincere gratitude to my advisor, Prof. Dr. Juergen Geis-Gerstorfer, for giving me this great opportunity to further my education. Also, thanks go to him for all his powerful support and encouragement.

I highly appreciate Prof. Dr. Heiner Weber for his care and help.

I would like to give special thanks to my co-workers Dr. Jun Chen, Dr. Lutz Scheideler and Dr. Frank Rupp for their cooperation and assistance.

Special gratitude is extended to Dr. Rudolf Reichl, NMI Natural and Medical Science Institute at the University of Tuebingen, Reutlingen, Prof. Oliver Eibl, Institute of Applied Physics, and Dr. Christoph Berthold, Institute of Geoscience, for their cooperation in XPS, TEM and XRD, respectively.

Sincere acknowledgement is also expressed to Prof. Dr. Dieter Kern and Dr. Thomas Altebaeumer for their support and cooperation.

10 Curriculum Vitae

Xiaolong Zhu

23.01.63	Born in Anhui, China

Education

1970 - 1974	Xiangyang Elementary School
1975 - 1978	Shengchong Middle School
1978 - 1980	Wangjiang High School No.1
1980 - 1984	Bachelor degree, Xi'an Highway University
1990 - 1993	Master degree in Materials Science, Harbin Institute of Technology
1993 - 1997	Ph.D in Materials Science, Harbin Institute of Technology

Work Experience

1984 - 1997	Assistant engineer, Hefei Bus Manufacturer
1990 - 1998	Engineer, General Research Institute for Non-ferrous Metals, Beijing
1997 - 1998	Postdoctoral fellow, University of Pretoria, South Africa
1998 - 1999	Associate professor, General Research Institute for Non-ferrous Metals, Beijing
1999 - 2001	Postdoctoral fellow, Kyungpook National University, Korea
2001 - 2002	Interchange scientist, National Research Lab (Gas Monitoring), Korea
2002 - 20005	Postdoctoral fellow, University of Tuebingen, Germany